

Master di II livello in "OPTICS AND QUANTUM INFORMATION"

Quantum Positioning Systems

Candidato Gianluca Di Ruzza Relatore Prof. Fabio Antonio Bovino

Anno Accademico 2022/2023

Summary

CH	APTEF	R 1	5
1	. Intr	oduction	5
	1.1.	Generalities on actual Global Navigation Satellite Systems (GNSS)	5
	1.2.	The Quantum Positioning System (QPS)	6
2	. Qu	antum active navigation system and key technologies	7
	2.1 Q	uantum active navigation system	8
	2.2 K	ey technologies of quantum active navigation system	8
3	.Quan	tum passive navigation system and its key technologies	12
	3.1 Q	uantum passive navigation systems	12
	3.2 K	ey technologies of quantum passive navigation system	13
	3.3 Q	uantum advantage vs conventional sensors	19
4	. The o	levelopment of quantum navigation technology	21
R	eferer	ces Chapter 1	23
CH	APTEF	₹ 2	25
1	. Intr	oduction to quantum entanglement and propagation issues	25
	1.1.	Experiments with Entangled Photons in Space	28
	1.2.	Entangled Photon Sources for Quantum Communications in Space	34
2	. Fur	ndamental Concepts	43
	2.1.	Quantum state vector	43
	2.2.	Density matrix	44
	2.3.	Quantum measurements	44
	2.4.	Encoding Quantum Information in Photons	46
	2.5.	Polarization states	46
	2.6.	Polarization measurement	48
	2.7.	Polarization entanglement	48
	2.8.	Bell's inequality	50
	2.9.	Bell-state fidelity	51
3.	Quan	tum Positioning System	52
	3.1.	Quantum entanglement preparation technology	55
	3.2.	Space optical communication and quantum satellite system	60
4 te		search status of quantum positioning and quantum clock synchronization	

78
78
82
88
91

CHAPTER 1

1. Introduction

1.1. Generalities on actual Global Navigation Satellite Systems (GNSS)

The accurate spatial information provided by constellations of satellites underpins the functioning of modern society. These sophisticated systems are collectively referred to as Global Navigation Satellite Systems (GNSS). A recent study has revealed that 85% of the information we process is related to space and time. Location services have a significant impact on a diverse range of industries, including location services, roads, aviation, maritime, and agriculture. There is a notable increase in forecasted demand, along with an expansion into autonomous vehicles and the Internet of Things (IoT) in general for cyberphysical systems and other advanced, high-accuracy positioning services. The most well-known system is the United States-led Global Positioning System (GPS), although there are other satellite-based systems in operation to a varying extent, including GLONASS, Galileo, Beidou and others. Despite the extensive utilisation of GNSS, particularly GPS, concerns pertaining to its accuracy and security have emerged as significant challenges in contemporary practical applications [1]. The United States' Global Positioning System (GPS) has comprehensive coverage of the terrestrial service volume, with a positioning accuracy of one metre and a time measurement accuracy of one nanosecond. The GPS system comprises approximately 24 satellites that orbit the Earth at a distance of approximately 4.25 Earth radii. In order to calculate the unknown user space-time coordinates (t_0 , r_0), four equations must be solved using the known satellite coordinates (t_s , r_s) and assuming line-of-sight signal propagation. The Global Positioning System (GPS) utilises a frequency range of 1575.42 MHz to 1227.6 MHz in the L-band for the transmission of its signals. In contrast, Russia's GLONASS system offers decametre-level positioning accuracy, 20-30 nanosecond time measurement accuracy, and superior anti-jamming capabilities compared to GPS. The Galileo system, which is currently under

construction, is comprised of 30 satellites that are situated in medium Earth orbit (MEO), and it currently exhibits a few-metre level of accuracy. Finally, China's Beidou system has been developed to achieve centimetre-level positioning accuracy. Satellite positioning systems (SPS) employ pseudo-range measurements to estimate the user's position. Range measurements are implemented by transmitting and receiving electromagnetic signals repeatedly, with the time biases between the satellite and receiver clocks calculated using a replicated pseudo-random noise. Clock synchronisation is crucial for the systems, with the precision of the arrival time measurement of light pulses dependent on it. The accuracy of positioning is limited due to the Heisenberg uncertainty relation. As the transmission power and bandwidth of the signal cannot be increased arbitrarily, the accuracy of traditional satellite positioning systems is difficult to improve in indoor, underground and urban environments, the continuous and accurate provision of GPS services is hindered by the potential for signal interruption and obfuscation. Furthermore, the security of GPS is also threatened by the potential for radio signals to be eavesdropped upon, rewritten, spoofed, jammed, or blocked. Consequently, the primary challenge for next-generation navigation technology is ensuring high availability and high credibility. In this context, a quantum technology-based navigation system may offer a potential solution. There is a growing interest in alternative Position, Navigation and Timing (PNT) solutions to GNSS worldwide, with numerous institutions and high-tech companies actively seeking effective solutions based on foundational research from academia (see [2], [3], [4], [5], [6], [7]).

1.2. The Quantum Positioning System (QPS)

The employment of quantum entanglement and squeezing techniques can facilitate the overcoming of the conventional limitations of classical methodologies, thereby enhancing the precision and efficacy of timing and localisation. The Quantum Positioning System (QPS) was initially proposed in 2001 by Dr. Giovannetti of the Massachusetts Institute of Technology (MIT) in the journal Nature. It has been demonstrated through mathematical calculation

that the characteristics associated with quantum entanglement and compression have the potential to enhance the precision of positioning. The preparation of a quantum entangled state and its subsequent transmission represent a significant advancement in the field of positioning technology. By eliminating the reliance on electromagnetic waves, the QPS is capable of surpassing the inherent limitations of traditional positioning techniques, while simultaneously offering enhanced confidentiality and anti-interference capabilities. Furthermore, the system exhibits a markedly reduced energy consumption in comparison to traditional alternatives. It is anticipated that the system will facilitate fundamental improvements in the miniaturisation, continuous working hours and stealth performance of the device.

In addition to satellite-based quantum active navigation systems, quantum passive navigation systems based on inertial navigation will also constitute an important means of exploring future navigation. In contemporary applications, inertial passive navigation is frequently employed in conjunction with satellite active navigation, thereby yielding enhanced outcomes. Furthermore, the passive navigation process does not exchange information with the external environment, thereby ensuring high credibility and high availability. This renders the passive navigation system a highly sought-after military application, particularly in the case of nuclear submarines and other crucial mobile targets that require the ability to conceal their position. This chapter primarily presents an overview of quantum navigation systems, encompassing their classification, fundamental technologies, and prospective developments. The subsequent chapter elucidates the essential technologies underlying quantum active position and navigation systems. The subsequent work presents the pivotal technologies underpinning quantum passive navigation systems. Finally, it delineates the prospective advancements of quantum navigation systems.

2. Quantum active navigation system and key technologies

QPS can be divided into two categories: quantum active navigation system and quantum passive navigation system. The quantum active navigation system adopts the method of transmitting and receiving quantum signals. The

positioning process usually uses satellite as the signal source. The quantum passive navigation uses quantum sensor device to locate, does not need external signals, and is usually positioned by detecting acceleration. The QPS employs the quantum entanglement and squeezing properties. Quantum information gain strong correlation and high density.

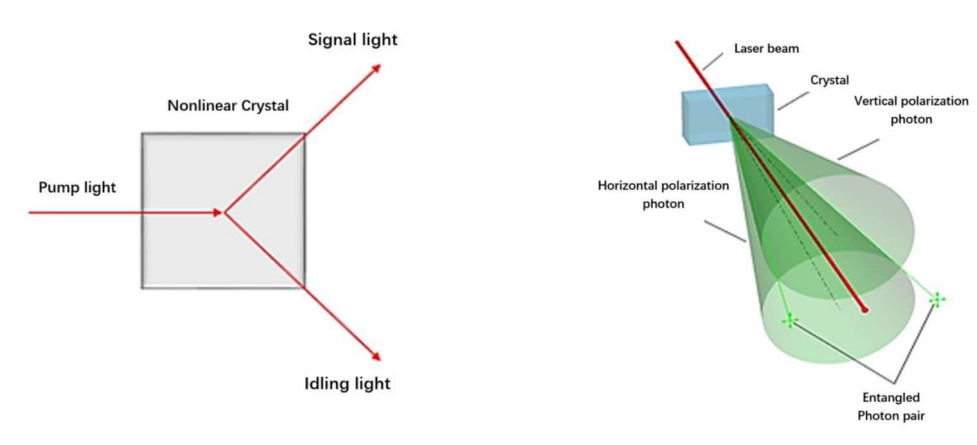
2.1 Quantum active navigation system

Active navigation system typically employs satellite-based ranging techniques. The fundamental theoretical principles underlying this approach were first articulated in 2004 by Dr. Bahder of the US Army Research Laboratory, who proposed an interferometric quantum positioning system. This model relies on a combination of techniques to prepare photon entanglement and track satellites, enabling the calculation of target position through a mathematical algorithm.

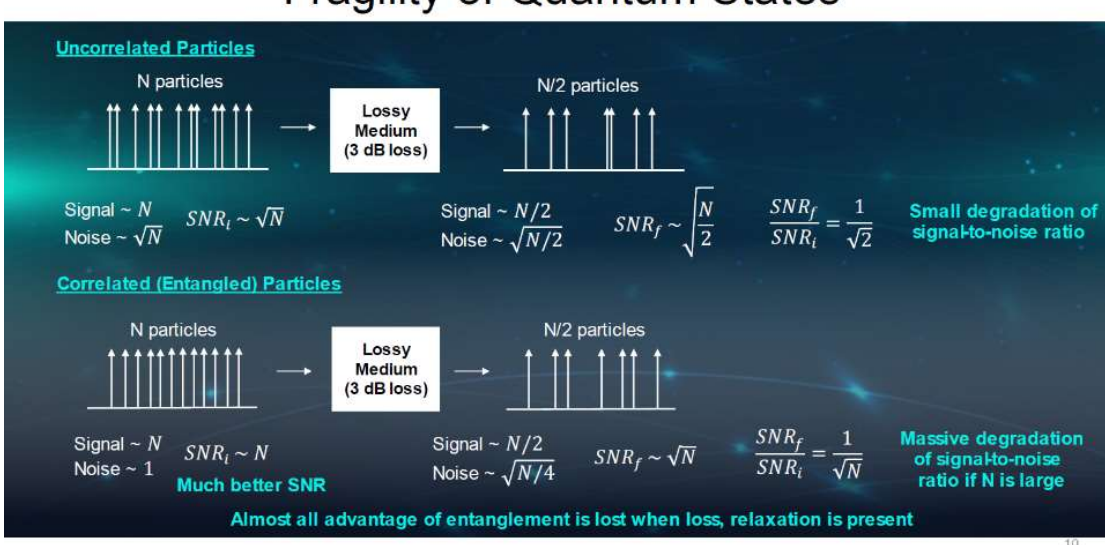
2.2 Key technologies of quantum active navigation system

2.2.1 Preparation of photon entangled states

Quantum satellite navigation systems necessitate the utilisation of a multitude of entangled photons throughout the ranging process. Currently, there are multiple techniques for generating entangled states, including the use of nonlinear crystals, ion traps, and atomic-optical cavities. The entangled state is prepared using the Spontaneous Parametric Down Conversion (SPDC) method. By passing a laser through a nonlinear crystal via the spontaneous parametric down conversion process of laser-pumped nonlinear optical crystals, the resulting twin photon pairs exhibit a high degree of entanglement purity.



Entangled states ensure better performances but are fragile (see figures above from [1] and below from [8]).



Fragility of Quantum States

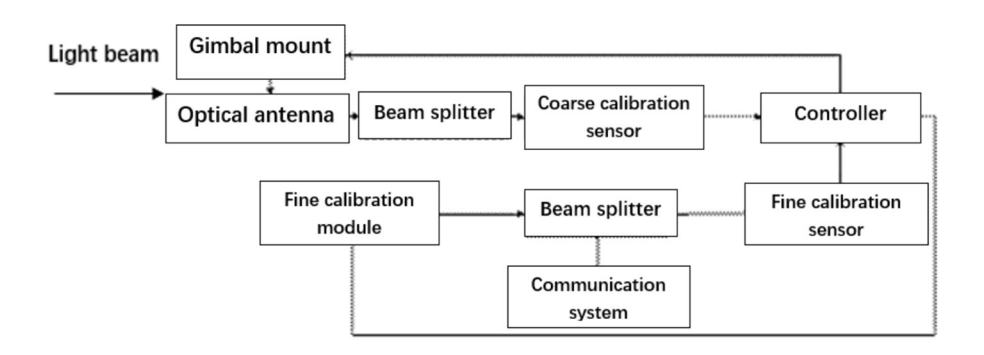
Figure from [8]

The preparation process is amenable to control and exhibits a discernible degree of stability. The second-order nonlinear effects observed in nonlinear optics allow for the possibility of splitting pump photons into a photon pair through scattering. The two photons comprising the photon pair may be designated as signal photons and idle photons, respectively. When the signal photon and the idle photon are in a state of polarisation perpendicular to the pump photon, an I-type association is formed. Conversely, when the polarisation state of the signal photon and the idle photon are perpendicular to each other, a type II association is formed. An ion trap is defined as a device that confines ions within a limited space by means of an electromagnetic field. The primary objective of studying the preparation of entangled states using ion traps is to achieve the entanglement of two or more atoms within a trapped ion system. This method has two principal advantages: firstly, the ions are confined within a highly vacuumed environment, which effectively isolates them from external influences, thereby prolonging their decoherence time. Secondly, the initial state

preparation and quantum state measurement exhibit a high degree of fidelity and efficiency, which is advantageous for quantum computing and quantum information processing. The study of the preparation of entangled states by cavity quantum electrodynamics (Cavity-QED) is gradually being carried out in conjunction with the development of cold atom technology and photoelectric testing technology. The electromagnetic field pattern trapped in the microcavity is either enhanced or suppressed by the boundary constraints of the cavity, thereby trapping the trapped atoms in a high-quality cavity and storing the quantum information in the atomic energy state. As a consequence of the coupling between the atoms and the cavity mode field, an interaction between the atoms and the light field is initiated. Consequently, the cavity system can be employed for the preparation of the entangled state of the atom and the light field. The current status of research into the preparation of entangled states can be summarised.

2.2.2 Capture, Tracking and Aiming Systems and Techniques

Furthermore, quantum satellite navigation systems necessitate the utilisation of spatial optical communication and the ATP technique, encompassing the processes of acquisition, tracking and aiming. The foundation of ATP technology is rooted in the methodologies of optical positioning, detection, and tracking, which are routinely employed in satellite laser communication. See figure below from [1]



The system's functions include the acquisition and high-precision tracking of beacon light transmitted by satellite communication terminals, as well as the high-efficiency, high-polarization-preserving reception of on-board quantum signal light. The challenges inherent to spatial ATP technology can be attributed to two key factors. One such requirement is that of high precision. In light of the impact of spatial loss on the bit error rate, the quantum light divergence angle in spatial scale quantum communication is typically in close proximity to the optical diffraction limit. Consequently, the beam must be aligned with a precision of micro radians (µrad). Additionally, the system is subject to external influences, including atmospheric channel loss, satellite platform interference, and the space thermal environment. An effective ATP system is capable of functioning optimally in such circumstances. The design of the ATP system incorporates a mechanical rotating platform that is coupled with an optical antenna, enabling the automatic adjustment of the received optical signal to guarantee the quality of the reception. Typically, the system's operational process encompasses two stages: coarse tracking and fine tracking. The coarse tracking stage captures the target within a broad range (approximately ±1° to ±20°). Following the capture, the aiming and real-time tracking precision of the target can be attained through the fine tracking system, with an accuracy of up to (1-10 µrad).

2.2.3 Quantum clock synchronization technology

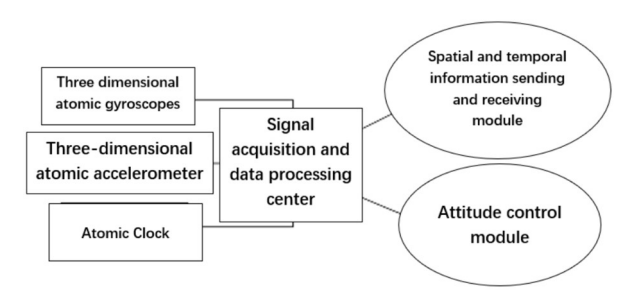
Quantum clock synchronisation is derived from the quantum entanglement of pairs of quanta, which may be photons or atoms. In quantum active navigation systems, the processes of positioning and clock synchronisation are two relatively independent operations. The discrepancy between the user's timekeeping device and the system clock, situated at the origin of the coordinate system, is determined with precision through second-order quantum coherence, after which the user device is calibrated to align with the system clock. The synchronisation process of satellite-based QPS is independent of the distance between the user clock and the system clock. Furthermore, as the two-photon coincidence count measurement of the Hong-Ou-Mandel (HOM) interferometer necessitates only a brief period of stability for the clock, the synchronization of

the user clock and the on-board clock is subject to only short-term stability requirements, with no long-term stability requirement. This simplifies the complexity of the hardware required on board. However, the system clock located near the origin of the coordinate system must have good long-term stability in order to maintain accurate system time over an extended period. A significant body of research on quantum clock synchronisation technology has been conducted in the past and is still ongoing.

3. Quantum passive navigation system and its key technologies

3.1 Quantum passive navigation systems

The quantum passive navigation system is an inertial navigation system. Similarly, to the conventional inertial navigation system, its ranging and timing functionality is not contingent upon the instantaneous reception of spatial satellite signals. The state adjustment and positioning are performed by means of inertial devices. This makes it an interesting and competitive alternative to GNSS. The principle of the quantum inertial navigation system is therefore to accurately locate the atomic inertia parameters after the atoms are disturbed. The quantum inertial navigation system has the same structure as the conventional inertial navigation principles. It is composed of four parts: a three-dimensional atomic gyro, an accelerometer, an atomic clock and a signal processing module. Some architectures also include a spatio-temporal information transceiver module and an attitude control module (see figure below from [1]).



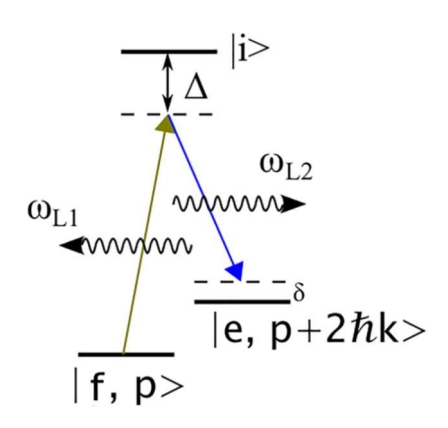
The core modules of a quantum passive navigation system include the atomic gyroscope, accelerometer and atomic clock. The performance of these modules

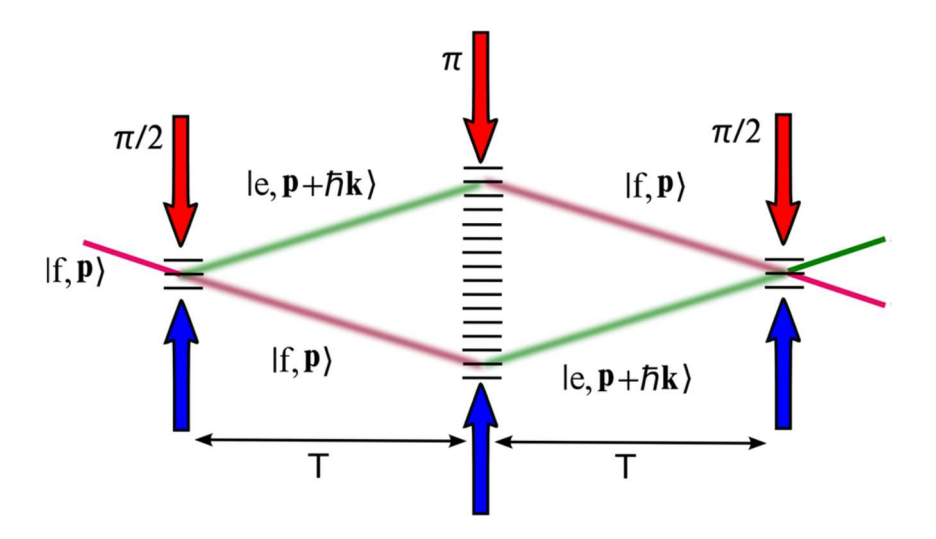
directly affects the system's positioning performance. The construction and experimental investigation of quantum passive navigation systems are ongoing areas of research.

3.2 Key technologies of quantum passive navigation system

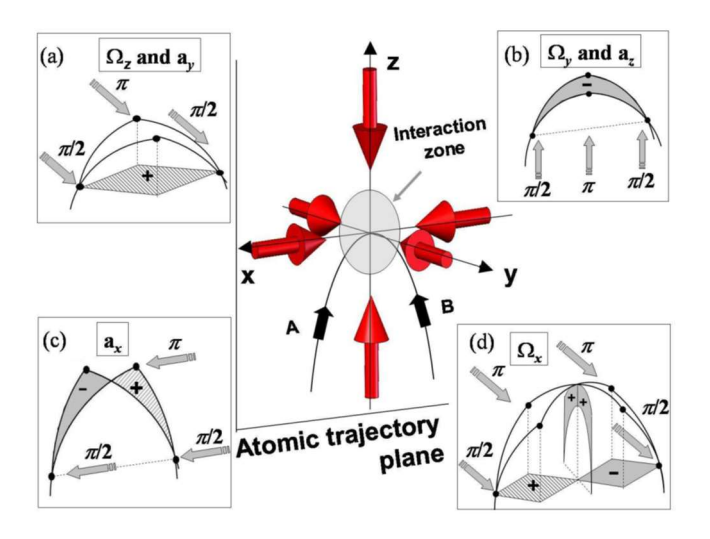
3.2.1 Atomic Gyroscope

Atomic gyros can be classified according to their operational principles, with the most common categories being atomic interference gyros and atomic spin gyros. They are both classified as inertial sensors. In essence, these devices rely on an optical interferometer, wherein beam splitters and mirrors are employed to alter the propagation mode of the light injected at the input port of the apparatus. Laser beams are employed to modify the propagation state of atoms in atom interferometry. Typically, these devices are implemented with stimulated Raman transitions, which are used to manipulate the atomic state. The Raman transition is a two-photon process in which the two laser beams interact with the atoms, which are described by the three-level system as illustrated in the figure below. This configuration is typical of a Mach-Zender configuration (figures both from [9]).





To determine the atomic phase Φ at the output of the AI, we measure the probability of detecting the atoms in states $|f,\mathbf{p}\rangle$, and $|e,\mathbf{p}+2\hbar\mathbf{k}\rangle$ which can be written as $P=A+Bcos(\Phi)$. For an apparatus subject to an acceleration \mathbf{a} , the phase Φ can be shown to be given by $\Phi_a=\mathbf{k}\cdot\mathbf{a}T^2$, T is the free propagation time between the laser pulses. If the device is subject to a rotation at an angular rate Ω , the atomic phase is $\Phi_\Omega=2\mathbf{k}\cdot(\Omega\times\mathbf{v})T^2$ where \mathbf{v} is the initial velocity of the atoms in the state $|f,\mathbf{p}\rangle$ at the AI input. The global inertial phase measured using an AI is therefore $\Phi=\Phi_a+\Phi_\Omega$ which thus contains information about both the rotations and accelerations to which the device is subjected. The free-falling atom interferometer is the most prevalent type of inertial sensor, particularly in confined environments. A six-axis inertial sensor is based on the following principle. The atomic clouds are launched on a parabolic trajectory and interact with the Raman lasers at the apex of the trajectory. The four configurations (a)-(d) provide access to the three rotations and the three accelerations, as illustrated in the figure below from references [9] and [10].



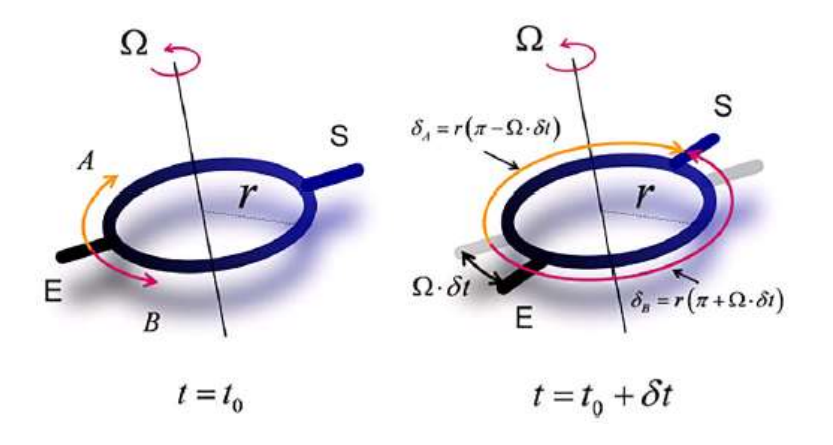
The atomic interference gyroscope is founded upon the atomic Sagnac effect. The cold atomic mass forms a cold atomic beam that follows the same parabolic trajectory in the opposite direction. The formation of an interference loop is induced by Raman laser stimulation, resulting in the phenomenon of double-loop atomic interference. The phase shift difference is therefore equal to half the phase shift caused by the rotation rate, which allows the rotation rate to be determined. For further information on the Sagnac effect in a circular guide, please

refer

to

reference

[9].



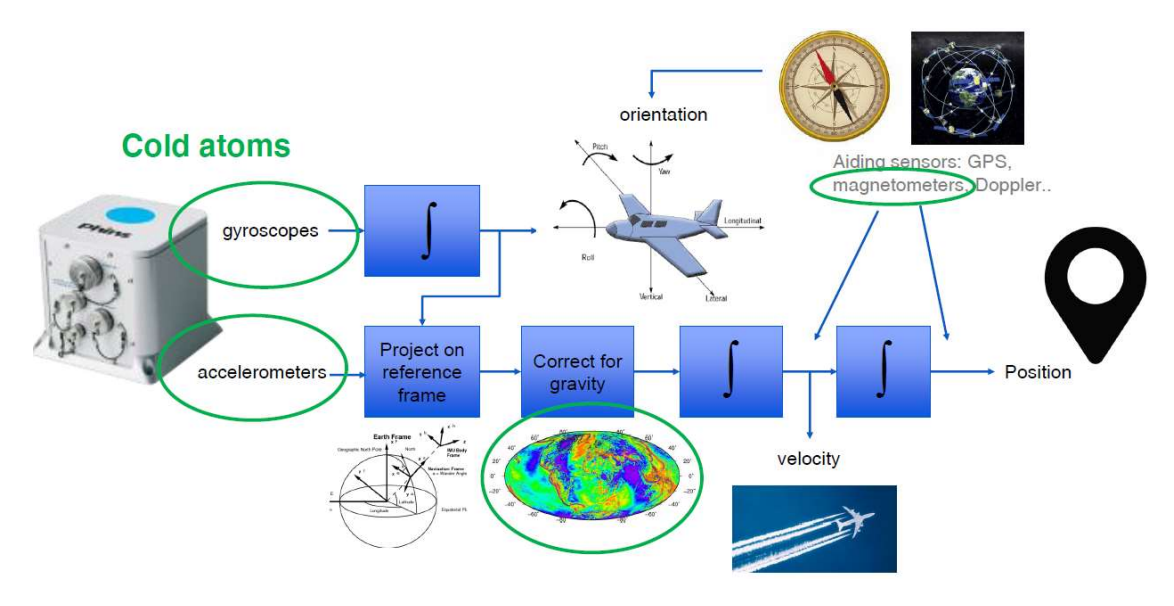
The theoretical value of the zero-bias drift of the atomic interference gyroscope is considerably lower than that of the traditional gyroscope. The theoretical precision is capable of reaching 1010 times that of an optical gyroscope. The atomic spin gyro employs the spin of an alkali metal atom's Larmor precession to achieve angular velocity sensing. At present, two principal approaches to

atomic spin gyros are in use: the nuclear magnetic resonance atomic spin gyro (NMRG), which employs the dual-nuclear method, and the atomic spin gyro operating in the spin-exchange less relaxation state (SERFG). In the 1960s, the United States initiated research on NMRG. Subsequently, a multitude of experiments have been conducted worldwide to investigate the behaviour of atomic gyroscopes, including the study of the effects of rotations on a cold atom interferometer mounted on a nadir-pointing satellite [11].

3.2.2 Atomic accelerometers

The discovery of the cold atom interference effect has been a catalyst for the development of atomic accelerometers, with the two fields often progressing in tandem. As stated in reference [12], cold-atom inertial sensors are dependent on laser cooling of atoms, without the necessity for cryogenic cooling. By irradiating certain materials with laser beams at frequencies proximate to atomic resonance, it is possible to capture atoms within the material. The atoms would lose their kinetic energy, resulting in a reduction in temperature to micro-Kelvin levels. The trapped atoms would exhibit quantum mechanical behaviour, allowing their states to be altered through the application of various techniques. In addition to the aforementioned implementation of the cold-atom technique through interference of wave functions, there are numerous other methods for employing this technique in inertial measurements. One potential approach is to release the trapped atoms from laser cooling, which would allow them to act as free-falling masses. Subsequently, the acceleration of the inertial sensor case can be quantified in relation to the aforementioned atoms. Nevertheless, alternative methodologies have been devised for the manipulation of trapped atoms, with a view to utilising them for the purposes of inertial measurement. It has been documented that the atoms can be set to a fixed velocity or guided for the purpose of conducting measurements pertaining to acceleration and rotation. However, cold-atom inertial sensors are distinguished by their high performance in comparison to typical optical gyroscopes, due to the fact that the effective atom wavelength is less than that of ring laser gyroscopes (RLGs) and fibre optic gyroscopes (FOGs) by ten orders of magnitude. Furthermore, the low

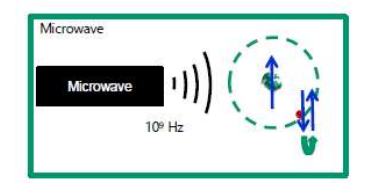
temperature of the trapped cold atoms results in low-noise measurements and a high signal-to-noise ratio (SNR) relative to optical inertial sensors. Quantum accelerometers exhibit performance that is several orders of magnitude superior to that of traditional inertial devices. To illustrate, if the position measurement error is less than 1 km after 100 days of sailing on a submarine, the submarine can perform long-term latency without satellite navigation. In recent years, there has been a significant amount of research conducted on atomic accelerometers. Gravity gradients have been measured with an accuracy of 1 m over a baseline length. Recently, atom interferometers have been employed in the development of these sensors. Since 2000, inertial quantum sensors (IQS) have been a subject of interest for ESA for space-borne applications, particularly using coldatom interferometry (CAI) [13]. For further information, please refer to the end-to-end quantum inertial solution presented in [14].

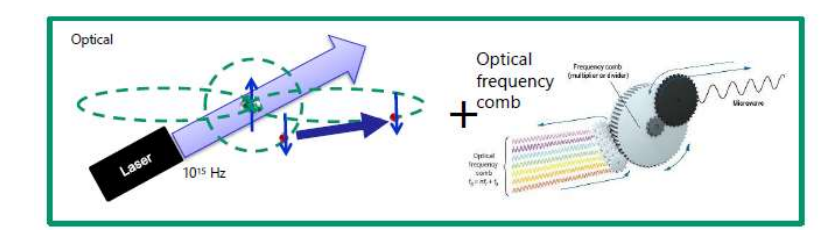


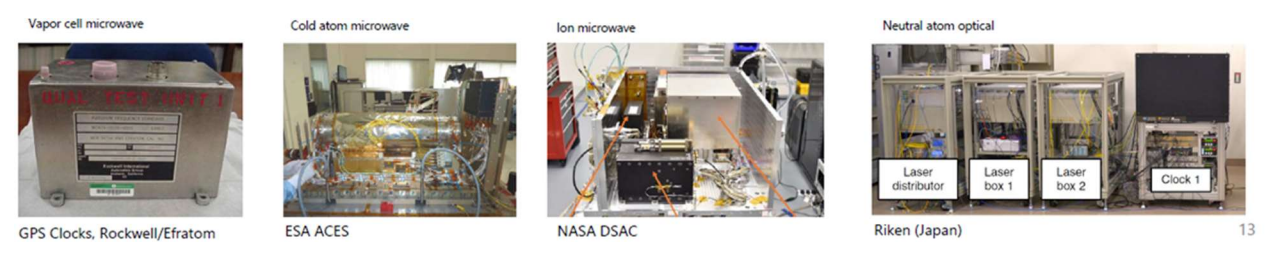
3.2.3 Atomic clocks

Quantum-mechanically defined energy levels in atoms

- Microwave clocks ns over hours, µs over days
- Optical clocks ns over days, µs over years







Figures from [8]

3.2.4 Quantum magnetometers

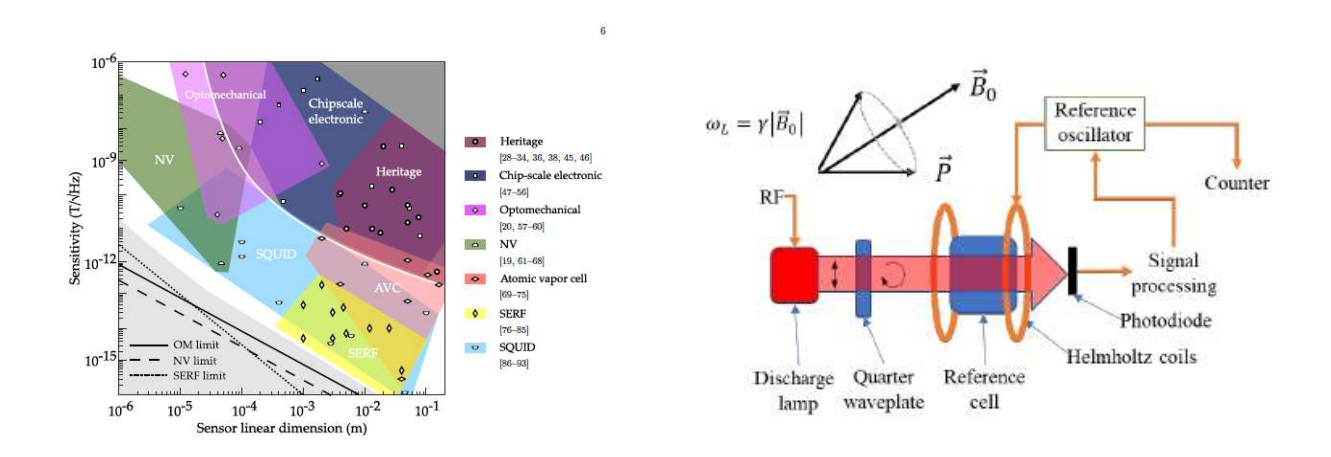
Magnetometers are also instrumental in navigation, employed primarily for two reasons:

• Attitude estimation: a multi-axes device is employed to measure the projection of the Earth's magnetic field. In three orthogonal directions, as a means of obtaining a three-dimensional estimation of the attitude within an Attitude and Heading Reference System (AHRS).

In geophysical navigation, measurements of the local magnetic field and its spatial variation are compared with known maps to correct the estimated position of the platform.

The sensitivity of the Earth's field is approximately pT.

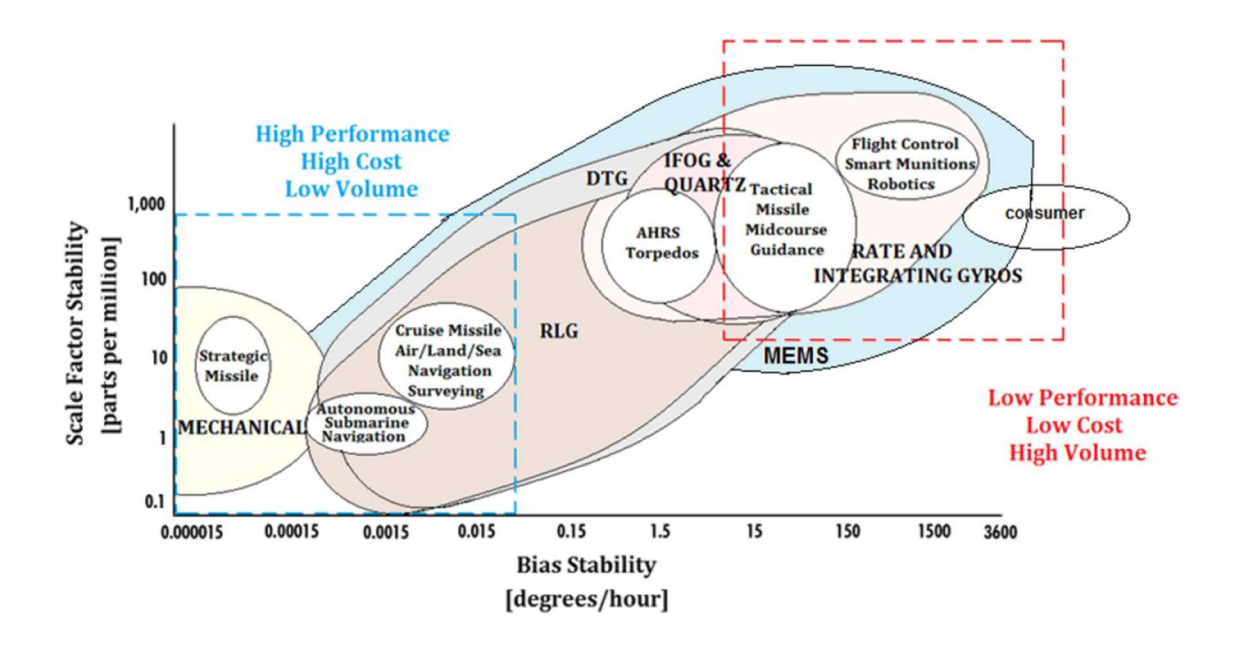
The sensitivity is low in low-field conditions, with a value of sub-fT.



3.3 Quantum advantage vs conventional sensors

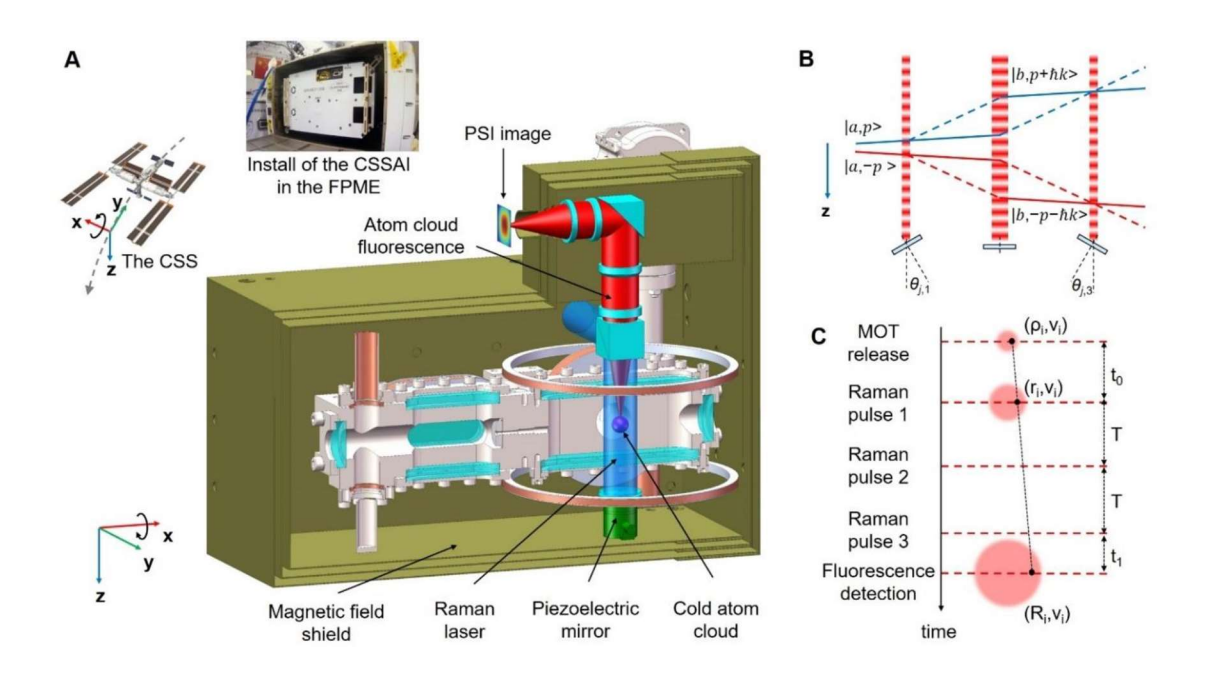
The superiority of quantum sensors over conventional sensors is clearly demonstrated in the tables below, which are referenced in sources [2] and [12]

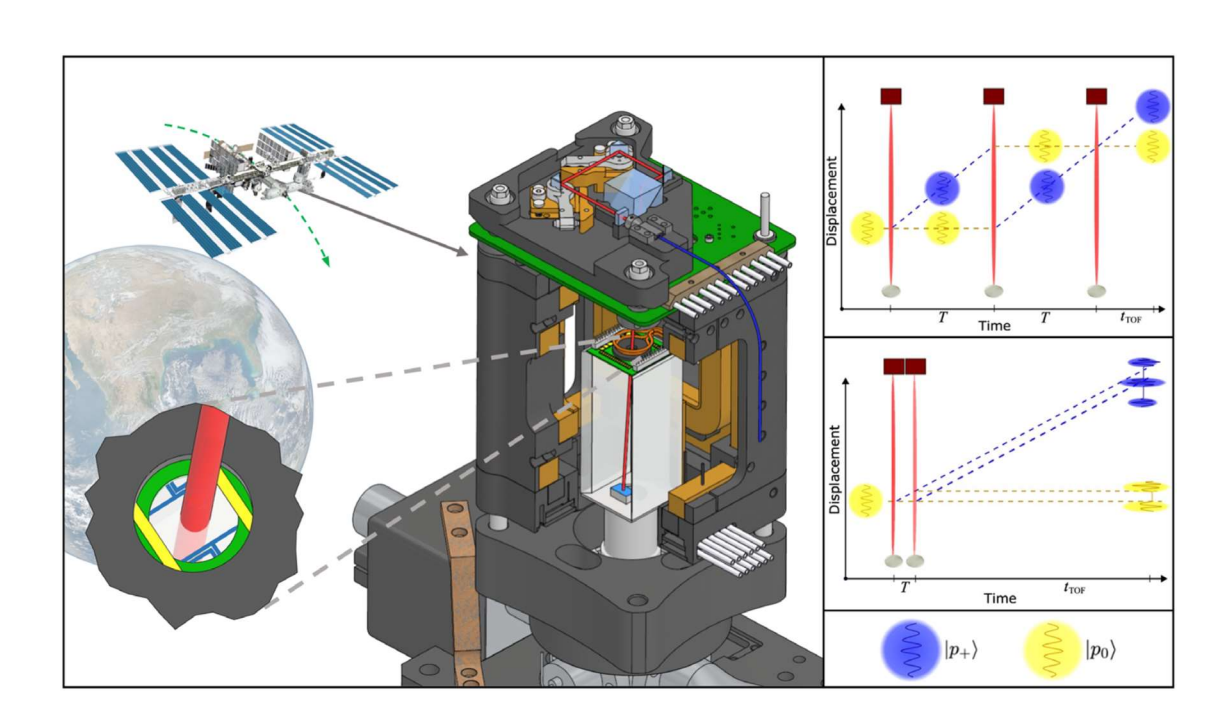
Technology	Quantum Performance	Conventional Performance
Acoustics	High resolution, low noise; Resolution: 1 mm	Resolution: 10 cm
Imaging	Sub-wavelength resolution; ultra low SNR Resolution: $< 1mm@10m$	Resolution: $\approx 1cm@10m$
Gravimeters	High sensitivity, low drift; Sensitivity: 50 nm/s ² ; Drift: 1 nm/s ² /hr	Sensitivity: 1 cm/s², Drift: 0.01 μm/s²/hr
Magnatamatawa	Ultra-high sensitivity $< 10^{-15}T$	Sensitivity: $\approx 10^{-12}T$;
Magnetometers	Very low noise $< fT/\sqrt{Hz}$	Noise $\approx pT/\sqrt{Hz}$
Gyroscopes	High stability, low drift;	Accuracy: up to 0.01°/hr;
Gyroscopes	Accuracy: $< 1e^{-6}$ /hr, Drift: $< 1e^{-6}$ /hr	Drift: up to 0.001°/hr
Accelerometers	High precision, low noise; Precision: 1 nm/s², Noise: 10 nm/s²	Precision: 10 nm/s², Noise: 100 nm/s²
Quantum Key Distribution	Unconditionally secure	Susceptible to eavesdropping and cybersecurity attacks
Clock Synchronisation	Frequency uncertainty: $< 10^{-18}$; Short term instability $< 10^{-17}$	Frequency uncertainty: $\approx 10^{-18}$; Short term instability $\approx 1 \times 10^{-16}$
Positioning Systems	Accuracy: 1 cm, global coverage	GPS: 1-5 m accuracy
Computation	Accelerated: >1000x speedup	Baseline (1x speed)



A number of innovative applications have emerged, including mobile cold atom interferometers that can be gyrostabilized on a boat or plane, as demonstrated by ONERA (see reference [14]), a quantum inertial navigation system developed by Infleqtion (see [15]), and magnetic navigation (MagNav) technology created by SandboxAQ (see [16]). Space applications atom interferometers have been exploited in space with the China Space Station

Atom Interferometer (ref. [17]) and the atom interferometer within the Cold Atom Lab onboard the International Space Station (ref. [18]), see figures below.



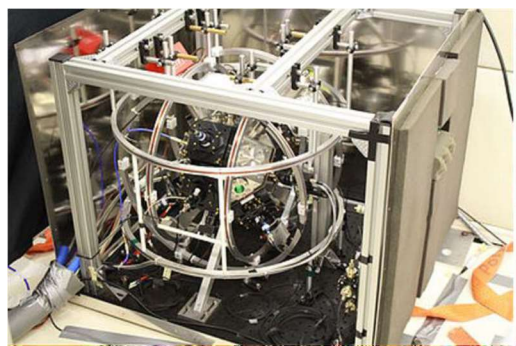


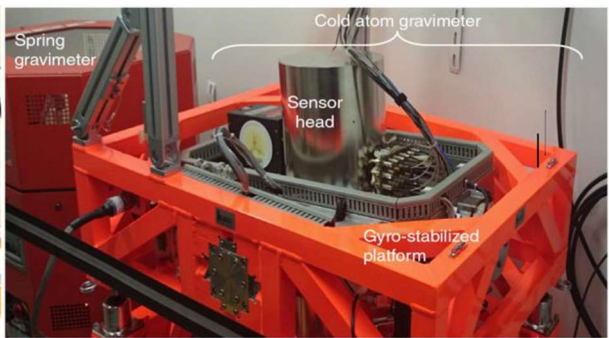
4. The development of quantum navigation technology

The quantum navigation technique employs the quantum properties of photons at the microscopic level, and is capable of exceeding the limits of classical measurement to achieve enhanced precision. It is a technology that is currently in its infancy but which shows great promise. The accelerated advancement of quantum information technology has facilitated the advancement of quantum device and quantum signal preparation, manipulation and storage-related technologies. The resolution of these technological challenges will provide robust engineering and technical support for the advancement of quantum navigation and positioning systems. In light of the limitations currently impeding the advancement of this field, it is imperative to not only conduct a comprehensive investigation into the pivotal technologies at hand, but also to address the following system-engineering challenge:

- 1. How can a comprehensive system framework be constructed? This chapter proposes a scheme for the preparation of an entangled state and a baseline for the erection of a system. The question thus arises as to how one might select the appropriate corner reflector, HOM interferometer, and counter-matching devices. The issue of anti-noise measures (loss of photons) and the protocols employed for multiple users must be addressed. The construction and testing of the quantum active navigation system are still in the theoretical phase, and the complete system framework has yet to be formed.
- 2. The question thus arises as to how the entangled state of spatial quantum signals can be maintained. The transmission of quantum signals in complex long-distance space environments presents a significant challenge, particularly in maintaining the coherence of entangled photons and the stability of quantum navigation systems. Optical communication in space exhibits superior precision and confidentiality compared to electromagnetic wave communication. However, it has become increasingly sophisticated and fragile. It follows that the optimal spatial optical communication system must meet more exacting technical specifications to guarantee the system's stability and ensure its optimal performance.

3. The question thus arises as to how quantum navigation can be combined with traditional navigation technology. Currently, the advancement of conventional navigation technology has reached a more advanced stage, whereas the development of quantum navigation and positioning technology is still in its infancy. It can therefore be predicted that the situation in which quantum navigation technology and traditional navigation technology coexist will become the norm for an extended period of time in the future. Despite the enhanced performance of quantum navigation and positioning, its implementation costs and technical complexity are significantly higher than those of traditional navigation. Consequently, traditional navigation can be fully applied to some areas where accuracy and safety are low, thereby allowing its advantages to be fully realised. It may be necessary to combine classical technologies with quantum systems as an intermediate stage on the path towards full-fledged quantum systems. Furthermore, the advancement of photonic integrated circuits (PIC) could potentially result in the reduction of the size of commercial systems. The objective of this thesis is to explore the utilisation of active Quantum Positioning Systems principles and architecture, which are based on satellites, optical and quantum principles. The foundational works that have informed this research are [19], [20] and [21]. The initial step towards enhancing Global Navigation Satellite Systems with optical technologies have been identified within [22]. Figures below are from [23]. Deeper discussion in the next chapter, referred to space-based QPS.





References Chapter 1

- [1] D. Feng (2018), Review of Quantum navigation
- [2] Olga Sambataro et al. (2021), Current Trends and Advances in Quantum Navigation for Maritime Applications: A Comprehensive Review
- [3] Shiqi Duan, Shuang Cong and Yuanyuan Song (2020), A survey on quantum positioning system, INTERNATIONAL JOURNAL OF MODELLING AND SIMULATION
- [4] E. Parker (2021), Commercial and military applications and timelines for quantum technology
- [5] Strategic Trade Research Institute, Centre for International and Security Studies at Maryland (2020), Position, Navigation and Timing: A Sectoral Composition Approach
- [6] H.R. Penney (2024), Mitchell Institute Policy Paper: The Quantum Advantage: Why it matters and essential next steps
- [7] UK National Quantum Strategy https://www.gov.uk/government/publications/national-quantum-strategy/national-quantum-strategy-accessible-webpage
- [8] Upendra N. Singh et al. (2024), NASA and external quantum sensing capability assessment for NASA Space-Base Science measurements
- [9] Carlos L. Garrid Alzar (2019), Compact chip-scale guided cold atom gyrometers for inertial navigation: Enabling technologies and design study
- [10] B. Canuel et al. (2006), 6-axis inertial sensor using cold-atom interferometry
- [11] Quentin Beaufils et al (2022), Rotation related systematic effects in a cold atom interferometer onboard a Nadir pointing satellite
- [12] Naser El-Sheimy, Ahmed Youssef (2020), Inertial sensor technologies for navigation applications: state of the art and future trends
- [13] Rainer Kaltenbaek et al (2021), Quantum technologies in space
- [14] Baptiste Battelier et al. NAVISP-El1-013: Quantum-based sensing for PNT. Final Presentation
- [15] UK Gov Press release: https://www.gov.uk/government/news/un-jammable-quantum-tech-takes-flight-to-boost-uks-resilience-against-hostile-actors
- [16] USAF Press release: https://www.af.mil/News/Article-Display/Article/3408951/magnav-project-successfully-demonstrates-real-time-magnetic-navigation/

- [17] Jinting Li et al. (2024), Realization of cold atom gyroscope in space
- [18] Jason R. Williams et al. (2024), Pathfinder experiments with atom interferometry in the Cold Atom Lab onboard the International Space Station, Nature communications
- [19] Thomas B. Bahder (2004), Quantum Positioning Systems
- [20] V. Giovannetti, S. Lloyd, and L. Maccone (2004), Quantum positioning system
- [21] V. Giovannetti, S. Lloyd, and L. Maccone (2021), Quantum enhanced positioning and clock synchronization
- [22] T. D. Schmidt et al. (2023) Optical Technologies for Future Global Navigation Satellite Systems.
- [23] NAVISP-EI1-013: Quantum-based sensing for PNT, Université Bordeaux (2021), Final Presentation. ONERA: Gyrostabilised onboard a boat and a plane. ICE: microgravity (parabolic flights) to prepare Space missions

CHAPTER 2

1. Introduction to quantum entanglement and propagation issues

The advent of quantum theory has precipitated a paradigm shift in our conceptualization of fundamental tenets such as realism and the locality of certain properties of physical objects.

In contrast to the behaviour of physical systems in classical physics, quantum systems are capable of existing in superposition states of mutually exclusive properties that are not defined until a measurement is made.

The extension of the superposition principle to multi-partite composite systems gives rise to another peculiarity of quantum theory, known as quantum entanglement.

In systems that are entangled, the physical properties of a composite system are shifted from its individual constituents to correlations between them. This results in non-local correlations between information carriers that may be separated by distance, which can be stronger than those permitted by any theory that assumes that quantum measurements merely reveal pre-determined local properties. This concept is referred to as local realism and has been empirically refuted for entangled systems through the violation of Bell inequalities.

The quantum superposition principle and quantum entanglement are not only of interest from a fundamental physics perspective, but also offer significant potential for technological advancement. The efficient generation, manipulation and transmission of quantum states are therefore of central importance in both experiments addressing the fundamental nature of the universe and the experimental realization of novel applications such as quantum-enhanced communication protocols.

The potential of quantum communications is significant, but it is accompanied by a challenge: quantum information is more susceptible to degradation than its classical counterpart. To ensure the reliable transfer of quantum information, it is essential to utilize information carriers that can be isolated from the effects of decoherence, which can be induced by interactions with an uncontrolled environment. The excitations of electromagnetic radiation modes, or photons, represent an especially promising system for the encoding of quantum information. They propagate at the speed of light and interact weakly with the environment, allowing for the coherent transmission of quantum information via optical fibres and free-space links. As in classical communications, it is convenient to encode quantum information in binary photonic degrees of freedom, which are referred to as 'qubits'. In the transmission of photons via fibres, qubits are typically encoded using the phase of photons (time-bin encoding), whereas orthonormal polarization mode encoding is commonly used in free-space links.

The distance over which photonic qubits can be transmitted with fidelity is ultimately constrained by the loss in the transmission channel and the noise in the single-photon detectors.

In classical fibre-optic communication, the use of amplifiers located along the transmission line can serve to mitigate the effect of loss. However, the nocloning theorem precludes the faithful replication of unknown quantum states.

Therefore, photonic qubits cannot be amplified in a straightforward manner, as is possible with their classical counterparts. This places an upper limit on the distance over which quantum information can be distributed via fibre-links at approximately 300 km. The deployment of quantum repeaters along the transmission line could potentially circumvent this limitation, thereby enabling the faithful distribution of quantum information without distance limitations. Nevertheless, they are still in the early stages of development. Quantum swapping has been trialled too.

An alternative option would be to transmit via atmospheric free-space links. At wavelengths in the near infrared, atmospheric absorption loss is significantly

lower than that of silica fibres. Link attenuation is mainly the result of beam diffraction and the limited aperture size of transmitting and receiving telescopes. Nevertheless, terrestrial free-space links necessitate a direct line of sight between the transmitter and the receiver, rendering them susceptible to obstruction and ultimately constrained by the Earth's curvature. It is therefore necessary to establish ground-to-satellite, satellite-to-ground, and inter-satellite links in order to fully benefit from free-space propagation. The deployment of quantum sources, relaying stations, and/or detection hardware on satellites would, for the first time, facilitate the implementation of quantum communication protocols on a global scale. Furthermore, it would provide unique opportunities for both fundamental tests of quantum theory at unprecedented distances and entirely new experiments aimed at a better understanding of the interplay between quantum physics and general relativistic physics. Although this may appear to be science fiction, a number of advanced experiments over longdistance free-space links, accompanied by several feasibility studies, have demonstrated that distributing quantum information via satellite links is a viable proposition with state-of-the-art technology. Consequently, a number of international research groups in Europe, Singapore, China, the USA and Canada are pursuing projects aimed at bringing quantum experiments to space,

marking the beginning of the quantum space race.

Distance (Lo- cation)	Experimental Achievement	Reference
0.6km (Vienna)	Long-Distance Free-Space Distribution of Entangled Photons	Aspelmeyer et al. 2003 [47]
7.8km (Vienna)	Distributing entanglement and single photons through an intra-city free-space quantum channel	Resch et al. (2005) [48]
13km (Hefei, China)	Free-Space Distribution of Entangled Photon Pairs over 13-km	Peng et al. (2005) [49]
1.5 km (Singa- pore)	Free-space Quantum Key Distribution with entangled photons	Marcikic et al. (2006) [50]
144 km (Ca- nary Islands)	Experimental Demonstration of Free-Space Decoy- State Quantum Key Distribution	Schmitt- Manderbach et al. (2007) [51]
144 km (Ca- nary Islands)	Entanglement-based quantum communication over 144 km	Ursin et al. (2007) [52]
6000 km (Matera)	Experimental demonstration of a quantum communica- tion channel from a LEO satellite to Earth	Villoresi et al. (2008) [42]
1.5 km (Water- loo, Canada)	Entangled quantum key distribution over two free-space links	Erven et al. (2008) [53]
350m (Singa- pore)	Daylight operation of a free space, entanglement-based quantum key distribution system	Peloso et al. (2009) [54]
144 km (Ca- nary Islands)	Transmission of entanglement over a 64-dB free-space channel	Fedrizzi et al. (2009) [55]
16 km (Huailai)	Experimental demonstration of free-space quantum teleportation	Jin et al. (2010) [56]
144 km (Ca- nary Islands)	Violation of CHSH inequality while closing freedom of choice loophole	Scheidl et al. (2010) [57]
143 km (Ca- nary Islands)	Quantum teleportation over 143 kilometres using active feed-forward	Ma et al. (2012) [58]
20 km (Ger- many)	Air-to-ground quantum communication with airplane moving at 290 km/h	Nauerth et al. (2013) [59]
1.6 km (Erlan- gen)	Atmospheric continuous-variable quantum communication	Heim et al. (2014) [60]
~ 0.7km (Wa- terloo)	Demonstration of three-photon quantum nonlocality	Erven et al. (2014) [61]

Table from [1]

1.1. Experiments with Entangled Photons in Space

The figure below illustrates a typical experimental scenario for the distribution of entanglement from a transmitter terminal to two receiver stations (Alice and Bob). Prior to initiating the transfer of quantum information, the transmitter is required to establish a conventional communication channel with Alice and Bob. This classical communication channel is subsequently employed to transmit data regarding the quantum state and the measurements performed on a specific pair, and constitutes an indispensable component of all quantum communication protocols. The quantum source, situated on the transmitter, is programmed to emit pairs of photons in a desired entangled state. The photon pairs display pronounced correlations in time and a high degree of entanglement

in the quantum information encoding degree of freedom. The individual photons that constitute each entangled pair are transmitted to Alice and Bob via free-space communication links, which are referred to as "quantum links." The photons are then collected via telescopes at the receiver terminals, where Alice and Bob each perform quantum measurements on their respective photons. The arrival time of each photon is recorded using single-photon detectors with high temporal resolution, and detection events comprising an entangled pair are identified based on their temporal correlations. The identification of photon pairs by their detection times necessitates that the transmitter and receiver modules establish and maintain a synchronized time basis. This can be achieved either by utilizing an external reference or autonomously via the classical communications link. Once the pair-detection events have been identified, Alice and Bob can reveal their stronger-than-classical correlations by communicating the outcomes of quantum measurements performed on each photon pair via the classical communications channel.

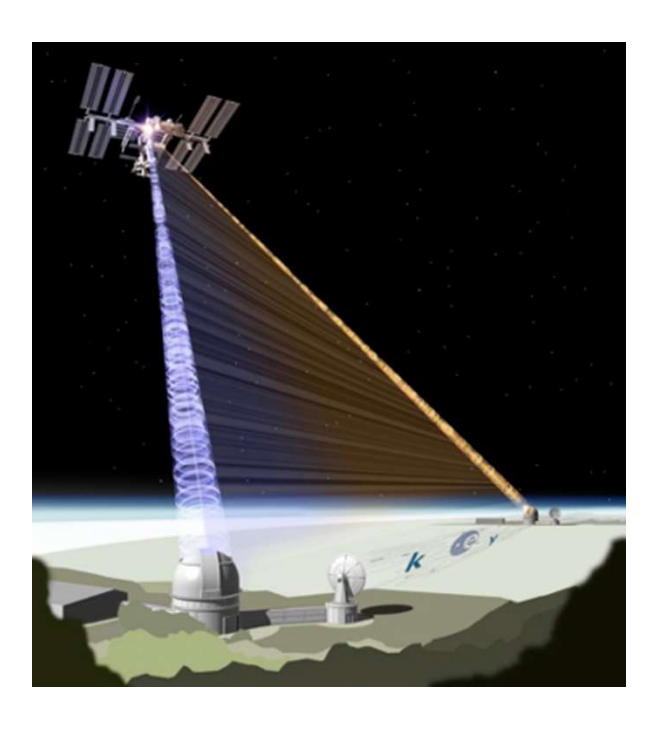


Figure from [3]

The distribution of entangled photon pairs over long-distance links and the revelation of their quantum correlations represents a significant technological challenge, particularly given the inevitable losses inherent to quantum links. These losses result in only a portion of the photons emitted by the transmitter reaching the receiver modules. The primary sources of loss along the optical transmission channel can be attributed to atmospheric absorption and scattering, on the one hand, and diffraction, telescope pointing errors, and atmospheric turbulence, which collectively result in beam broadening and, consequently, a reduction in the fraction of photons collected by the receiver aperture.

In order to achieve experimentally feasible pair-detection rates, it is necessary to emit a large number of photon pairs from the transmitter, as well as to minimize losses in the transmission channel (for example, through the use of advanced tracking techniques in order to minimize beam wander and telescope pointing errors) and in the receivers (for example, through the use of efficient single-photon detectors). It should be noted that, since correlated photon pairs are identified by their arrival times, there is an upper limit to the effectiveness of the source rate in mitigating against link loss. Once the average time between two successive pair emissions at the source is reduced to a level below the timing resolution of the detectors and/or the precision of the respective clock synchronization, successive pairs emitted by the source can no longer be distinguished, resulting in an increased number of so-called accidental coincidence counts. These accidental coincidences originate from uncorrelated photon pairs, which consequently reduce the quality of the observed entanglement.

Furthermore, the quantum correlations of the attenuated photon streams arriving at the receiver modules are obscured by the detection of uncorrelated background photons and intrinsic noise in the single-photon detectors (dark counts). Consequently, attaining an acceptable signal-to-noise ratio (i.e. fringe visibility) necessitates the isolation of entangled photons from spurious background counts. This can be accomplished through the utilization of narrowband spectral filters (passband <1nm), spatial filtering (i.e. minimizing the

detectors' field of view), and temporal filtering techniques. However, this in turn requires precise and stable timing synchronization of transmitter and receiver modules.

Furthermore, the detection of the desired quantum correlations necessitates the continuous emission of photons by the transmitter in a well-defined, maximally entangled state, as well as the continuous compensation for transformations induced by changes in the quantum links, receivers, and transmitter.

1.1.1. Mission scenario for quantum entanglement in space

The installation of quantum transmitter and receiver modules on space platforms will facilitate a diverse range of experiments in space. The current conceptualization of experimental scenarios entails the utilization of transmitter/receiver modules in both space and on the ground, facilitating the distribution of quantum entanglement from the ground to satellites situated in low Earth (LEO), mid Earth (MEO), or geosynchronous orbit (GEO). Additionally, the transmission of entanglement can be directed from satellites in GEO/LEO/MEO to the ground, or via inter-satellite links (ILS). It is also conceivable that future missions may extend to scenarios involving links between the Moon and Earth or Mars or deep Space, with a suitable source of entangled photons placed symmetrically or asymmetrically between the two receiving locations.

Long-term projects may also entail the utilization of quantum relaying satellites, which would be capable of performing Bell-state analysis on photons received from independent entangled photon sources (entanglement swapping). The deployment of relaying stations equipped with quantum memories would facilitate the establishment of a satellite-based quantum repeater infrastructure, potentially extending the reach of quantum communications to unprecedented distances. Nevertheless, in order to perform a Bell-state analysis on photons from independent sources, it is necessary that the photons received be indistinguishable in time. This implies that the arrival time of the photons must be synchronized to within the coherence time of the photons. This can be achieved either by synchronizing the generation of pairs in the two sources, or with sources that have extremely long coherence times (i.e. narrow bandwidth)

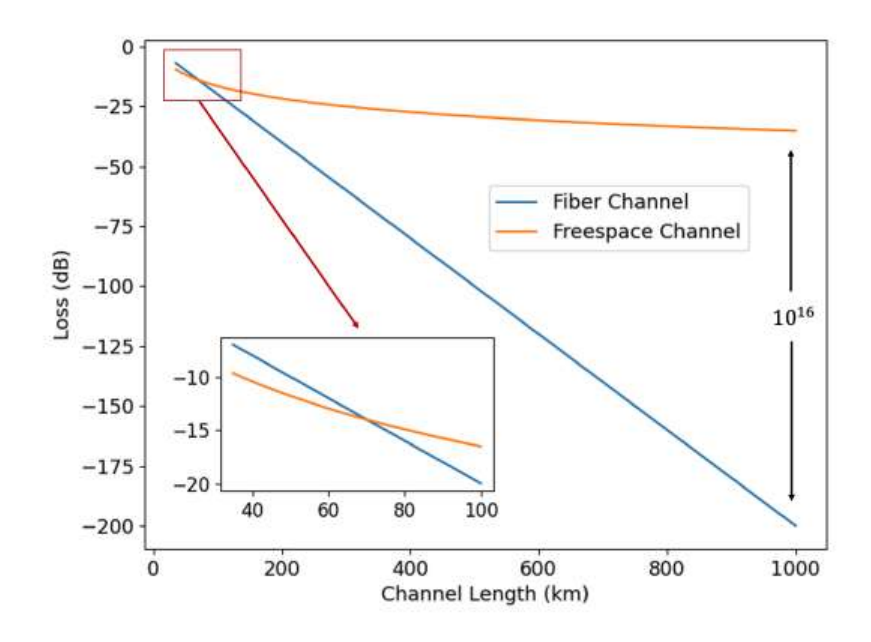
and ultra-fast detectors. Nevertheless, the considerable technological challenge associated with the construction of a relaying station, coupled with the fact that quantum memories are still in the early stages of development, renders such a scenario highly improbable in the near future.

1.1.2. Expected link loss in various mission scenarios

The Table below lists the estimated losses in quantum communications links between ground and satellites in LEO (\sim 500km altitude) and GEO (\sim 36000km altitude) for various scenarios.

800nm 1550nm	ground- based receiver	LEO re- ceiver	GEO receiver
ground-	:=	27.4dB	64.5dB
based transmitter		26.3dB	63.4dB
LEO trans-	6.4dB	28.5dB	52.9dB
mitter	12.2dB	33.6dB	58.6dB
GEO trans-	43.6dB	52.9dB	53.9dB
mitter	49.3dB	58.6dB	59.7dB

Table from [1]



Typical losses in fibre vs free-space channels.

The attenuation parameter of fibre is ~ 0.2 dB/Km (Table from [2])

It is notable that the loss in satellite-to-ground links is considerably less than that observed in ground-to-satellite links. This asymmetry can be attributed to the differing impact of turbulence in the lower atmosphere on the two cases. Turbulent layers in close proximity to the emitter result in more severe beam distortions than those in close proximity to the receiver telescope (so-called shower curtain effect), which leads to a larger effective beam diameter and correspondingly higher link loss. It is evident that quantum communications with satellites is feasible in a multitude of configurations. Although maintaining a link with a low Earth orbit (LEO) satellite is more challenging than with a geosynchronous Earth orbit (GEO) satellite, the significantly lower loss for both uplink and downlink scenarios, together with the lower costs of launching a dedicated LEO satellite, suggest that the first proof-of-principle experiments will involve LEO-to-ground, or ground-to-LEO links.

1.1.3. Proposals for quantum experiments with in-orbit satellites

A substantial number of experiments have been conducted, or are scheduled to be conducted, in orbit. These experiments span a range of fields, from fundamental physics tests with quantum technologies in space, such as the Einstein Equivalence Principle, to search for dark matter and dark energy, or the interface between quantum physics and relativity, to space-based gravitational wave detectors (see [2]). The exploitation of quantum key distribution (QKD) has recently become a topic of interest. The QUESS experiment, which involved the Chinese low Earth orbit (LEO) satellite Micius, became the inaugural space-based quantum communication mission to be launched and has since undergone further developments. It has demonstrated the distribution of entanglement to two ground stations separated by approximately 1,200 km, ground-to-satellite quantum teleportation over distances of up to 1,400 km, and the realization of a hybrid quantum communication network with a total quantum communication distance of 4,600 km. Furthermore, the potential of quantum technology has been explored in the

context of enhanced communication, timing and synchronization, deep space communication and the development of a quantum internet. Additionally, proof-of-principle experiments and the implementation of cold atoms and atom-based clocks have been conducted.

1.2. Entangled Photon Sources for Quantum Communications in Space

The generation of entangled photon pairs in a laboratory setting has become a standard procedure for experimentalists worldwide. Currently, research and development efforts are primarily focused on enhancing the performance characteristics of the sources.

The quality of an entangled photon source is typically evaluated based on three key parameters: brightness (quantified as the number of generated pairs per milliwatt of pump power), spectral bandwidth, and the purity, or visibility, of the entangled state.

A number of schemes for the generation of photon pairs exist, but at present the most widely used and versatile method is spontaneous parametric down-conversion (SPDC) in second-order nonlinear crystals. Recent developments in the field have resulted in a rapid increase in source efficiency over the past few years, as illustrated in the figure below, which depicts the development of source brightness over time.

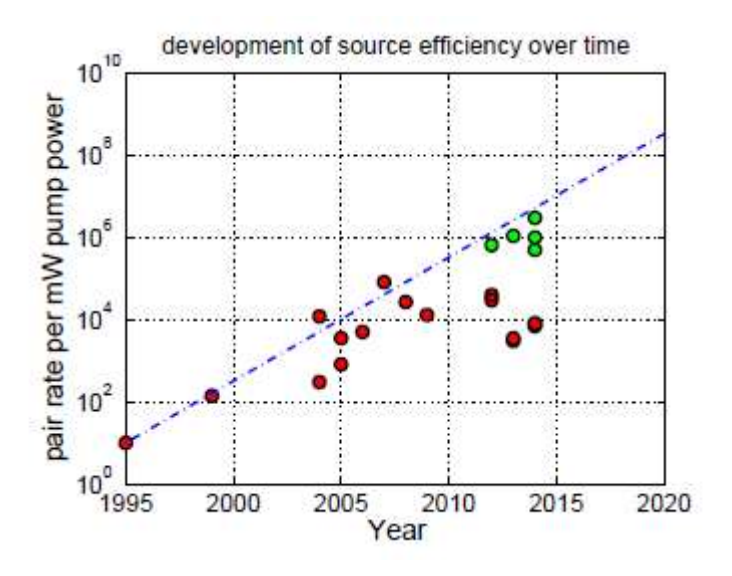


Figure from [1]

While many sources of entangled photon pairs have been shown to work well under laboratory conditions, the requirements for misalignment tolerances, mechanical stability and temperature control remain high. Improving long-term stability and robustness, while maintaining a compact footprint and minimizing power consumption, are key challenges to be addressed in the development of space-qualified sources of entangled photons. However, as experiments using entangled photons are rapidly expanding into other fields of research, such as biology and telecommunications, the interest in field-deployable sources is not limited to space applications. Additional criteria that need to be addressed in order to extend the use of entangled photons beyond quantum optics laboratories and enable potential commercial applications are ease of operation and the number, cost and complexity of optical components required to build the source. The figure below lists a number of factors that have influenced the design parameters chosen for the sources. These are discussed in more detail in the following sections.

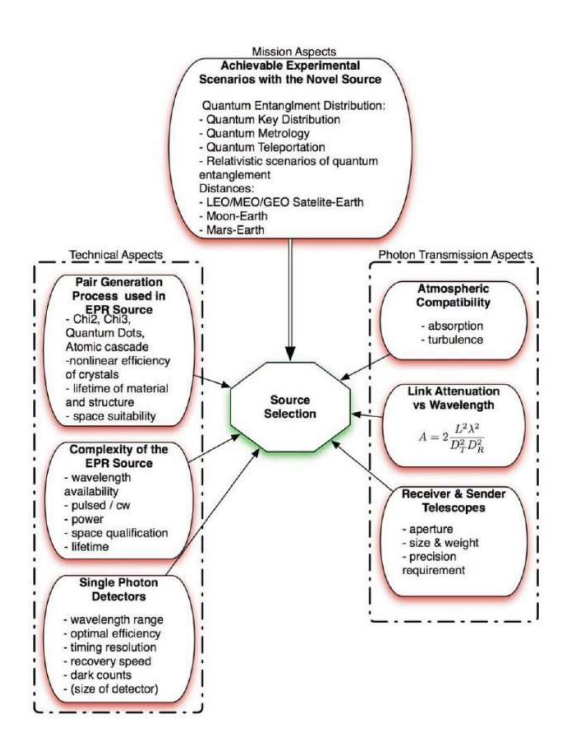


Figure from [1]

1.2.1. Encoding quantum information

Quantum information can be encoded in different degrees of freedom of photons. A number of possible approaches are listed in the table below, together with a brief discussion of their advantages and disadvantages with respect to free-space applications.

Degree of free- dom	Behavior in free-space link	Experimental advan- tage	Experimental challenge
Polarization	Well-tested under turbulent atmospheric conditions.	Detection and manip- ulation (wave plates) straightforward. Po- larization correlations independent of spatial mode.	Alignment and temperature- dependence of bire- fringent elements in sender and receiver. Requires compensation of relative rotations of the sender and receiver.
Relative phase/time- bin	Not tested under turbu- lent atmospheric condi- tions, but should work in principle.	Only one polarization required, possibly of relative orientation.	Active stabilization of two unbalanced inter- ferometers at the source and the receivers. High visibility only in single spatial mode.
Spatial mode	Not expected to work well under strong turbulent atmospheric conditions due to wave-front distortion.	No polarization depen- dence. High dimen- sionality (channel ca- pacity).	Perfect compensation of wave-front distor- tions, and accurate pointing required.
Continuous Variables (quadrature encoding)	Has been demonstrat- ede under turbulent at- mospheric conditions.	Robust with respect to background. Sources and detection modules well-developed from classical communica- tions.	Loss-tolerance cur- rently below antic- ipated efficiency of free-space satellite link.

Table from [1]

This chapter explores the use of polarization as a means of encoding quantum information. This approach has been selected due to the resilience of polarization qubits to the effects of atmospheric turbulence, which can otherwise compromise the integrity of transmitted data. Moreover, polarization qubits can be readily detected and manipulated with only basic optical instruments, such as wave plates and polarizers. These devices are likely to be space-qualifiable, making them compatible with both ground-based and space-based detection modules and sources.

One of the principal challenges associated with the utilization of optical elements in harsh operational contexts is their temperature-dependent birefringence. This issue could be resolved by thermalizing the optimal design through the incorporation of an appropriate combination of birefringent materials.

1.2.2. Pair-generation mechanisms

A source of polarization-entangled photons suitable for use in a space suit must be capable of reliable and highly efficient pair generation. The current gold standard for generating polarization-entangled photon pairs is spontaneous parametric down-conversion (SPDC) in nonlinear materials, which is the most mature method in this field. This renders SPDC the most viable candidate for incorporation into the inaugural generation of space-based applications. Nevertheless, in the long term, alternative emerging technologies, most notably four-wave mixing in nonlinear fibres and solid-state sources, are likely to become promising candidates for further improvements in terms of performance.

Spontaneous parametric down-conversion (SPDC) is a quantum mechanical process that occurs in non-centrosymmetric second order nonlinear crystals (e.g. BBO, LBO, KTP, or LN). In this process, a strong pump field (p) can induce the spontaneous emission of two lower-energy photons, which are commonly termed signal (s) and idler (i) photons. In contrast to an ideal 'photon pair gun' that generates photon pairs in a deterministic manner, SPDC is a fundamentally probabilistic process, exhibiting typical photon pair generation probabilities of less than 10⁻⁹ per pump photon. Consequently, the signal and idler fields are in their respective vacuum states the majority of the time. It is only after their detection (post-selection) that the correlations of entangled photon pairs can be revealed. Given the random nature of the emission process, there is always a finite probability of emitting more than one photon pair within a given time window. This results in accidental coincidence counts, which impair the quality of the entangled two-photon state. Notwithstanding these constraints, probabilistic pair generation via SPDC remains the most prevalent approach, largely due to the process's relative simplicity and versatility.

A plethora of distinct two-photon quantum states can be generated with high visibility quantum correlations in a multitude of degrees of freedom. This has enabled the performance of fundamental tests of quantum theory and the implementation of diverse applications in quantum optics.

The distinction between type-0, type-I and type-II SPDC is dependent on the polarization of the interacting fields. Type-I and II processes involve orthogonally polarized fields, whereas in type-0 processes all photons are co-polarized.

In the initial generation of type-II SPDC-based sources, correlations in energy and momentum were employed to generate polarization-entangled photons within constrained spatial regions. The pair-collection efficiency was enhanced by overlapping the type-I emission cones from distinct crystals. However, the configuration was constrained to relatively short crystals due to the non-collinear nature of the setup. A substantial enhancement in the pair rate was attained with a collinear non-degenerate configuration, which permitted the entangled photons to be effectively coupled into single-mode fibres.

The latest advances in waveguide technology also offer a promising avenue for the development of fully integrated sources of entangled photons based on SPDC, with the potential for significantly enhanced pair generation efficiency. A fully integrated solution is a highly attractive proposition, as it has the potential to significantly reduce mechanical stability issues. Nevertheless, the potential for a significant reduction in size (including temperature control and electronics, etc.) is unlikely to be realized in comparison to a well-designed bulk optics solution.

Presently, sources based on SPDC in bulk crystals are the most suitable option for meeting the challenging performance requirements in terms of versatility, stability, fibre-coupling efficiency, visibility, and pair-detection rates for application in high-loss free-space links.

Four-wave mixing (FWM) is a third-order nonlinear process, in which two pump photons of a strong pump laser spontaneously produce a signal and idler pair. Four-wave mixing is mediated by the third-order nonlinearity $\chi^{(3)}$, which occurs naturally in a number of optical materials, particularly waveguiding structures such as single-mode fibres, highly nonlinear photonic-crystal fibres, and nanoscale silicon waveguides. In-fibre sources based on four-wave mixing can exhibit high brightness and ultra-narrow bandwidths due to the long interaction lengths and the confinement to a single spatial mode. The achievement of high-fidelity polarization entanglement in a fibre Sagnac geometry represents a

significant advance, with an all-fibre solution offering considerable advantages in terms of mechanical stability. One significant drawback of four-wave mixing is the high level of linear background noise that arises due to spontaneous Raman scattering. Currently, the attainment of high signal-to-noise ratios is most frequently accomplished at low temperatures and with picosecond-pulsed pump sources. Nevertheless, fully integrated on-chip sources with suitable input and output coupling are likely to become a viable solution in the near future. Solid-state sources represent a promising avenue for the generation of

Solid-state sources represent a promising avenue for the generation of entangled photon pairs on demand. In solid-state sources, an excitation pulse prepares a quantum dot in a biexciton state, which is a configuration of electron-hole pairs with opposite spins. As the electron-hole pairs recombine, two photons are emitted as a result of one of two possible relaxation cascades. The circular polarization of the emitted photons is anticorrelated due to the conservation of spin. If the two relaxation channels can be made indistinguishable, the procedure yields a pair of photons in a maximally polarization-entangled state. In contrast to spontaneous parametric processes, the biexciton decay results in the generation of triggered photon pairs, with two photons per excitation pulse in an ideal quantum dot.

The primary limitation of solid-state sources is the relatively low entanglement visibility, which has been observed to be approximately 70%. This is a consequence of structural imperfections, which result in a polarization-dependent intermediate exciton level and lead to decoherence of the entangled state. A further limitation of solid-state sources is that they currently require operation at cryogenic temperatures (less than 20K). The on-demand generation of photon pairs is undoubtedly a significant advantage of solid-state sources over those based on spontaneous parametric processes. However, for solid-state sources to become a viable alternative to SPDC, it will be necessary to overcome the difficulties associated with the repeatable production of symmetric quantum dots and to demonstrate a higher degree of entanglement.

1.2.3. Wavelength considerations

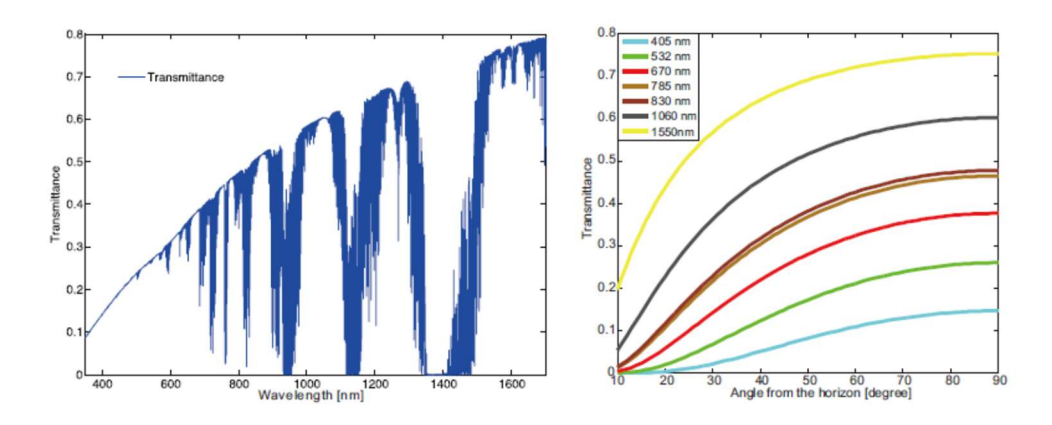
The optimal operational wavelength for space-suitable entangled photon sources is contingent upon a number of factors, including the availability of atmospheric transmission windows, the efficiency with which single photons can be detected, the diffraction of beams, and the accessibility of space-proof optical components. Additionally, the wavelength range that can be addressed via the SPDC process must be considered.

1.2.4. Single-photon detectors and optical components

The majority of experiments utilizing polarization-entangled photon pairs are conducted within the wavelength range of 700-850 nm, or in the telecommunication windows centred around 1300 nm and 1550 nm. The initial wavelength range is primarily driven by the responsivity of silicon-based single-photon avalanche diodes (SPADs) within this region. Moreover, space-qualified silicon SPADs have already been demonstrated. Currently, there are numerous initiatives aimed at enhancing photon-counting technology and methodology.

1.2.5. Atmospheric transmission windows

As the most probable mission scenarios entail free-space transmission through the Earth's atmosphere, the atmospheric transmission properties constitute an additional factor that must be taken into account. Specifically, within the responsivity range of silicon and InGaAs SPADs, the bands 400nm-650nm, 730nm-750nm, 770nm-870nm, 1000nm-1 The 100 nm, 1170 nm-1300 nm, and 1500 nm-1700 nm ranges are free of strong absorption resonances, exhibiting a slight increase in transmittance as the wavelength increases. See below the simulated atmospheric transmittance for zenith with different wavelengths (left) and different altitude angles (right), from [3]



1.2.6. Diffraction and turbulence

The effective aperture of receiving telescopes gives rise to a further loss mechanism, namely beam broadening due to diffraction and atmospheric turbulence. The utilization of shorter wavelengths and/or larger diameter transmitter telescopes can serve to minimize diffraction loss. However, this phenomenon becomes the primary source of loss for inter-satellite and satellite downlink experiments. It should be noted that in an uplink scenario, atmospheric turbulence becomes the dominant factor when the diameter of the transmitter extends beyond a certain length, thereby limiting the extent to which increasing the sender aperture can mitigate diffractive broadening.

1.2.7. Pump Sources for SPDC

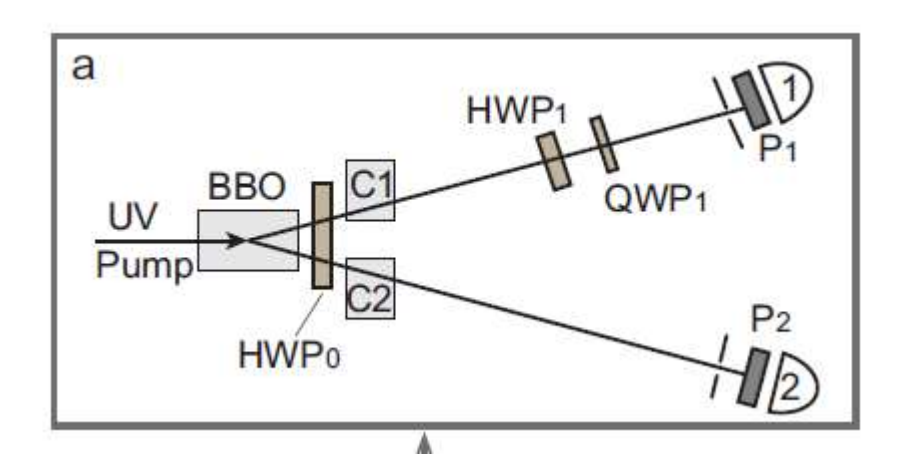
A plethora of laser technologies are capable of producing coherent radiation that is suitable for pumping the SPDC emission process. Semiconductor laser diodes (LD) are the optimal choice, as they offer a well-balanced trade-off between complexity, volume occupation, and performance.

Laser diodes are not currently available in wavelengths below 400 nm. Therefore, the wavelength of the signal and idler photons generated via SPDC must be centred around wavelengths above 800 nm. Generation of shorter wavelengths could be achieved by doubling the frequency of the radiation emitted by a 700 nm LD pump, but this would entail a considerable increase in complexity.

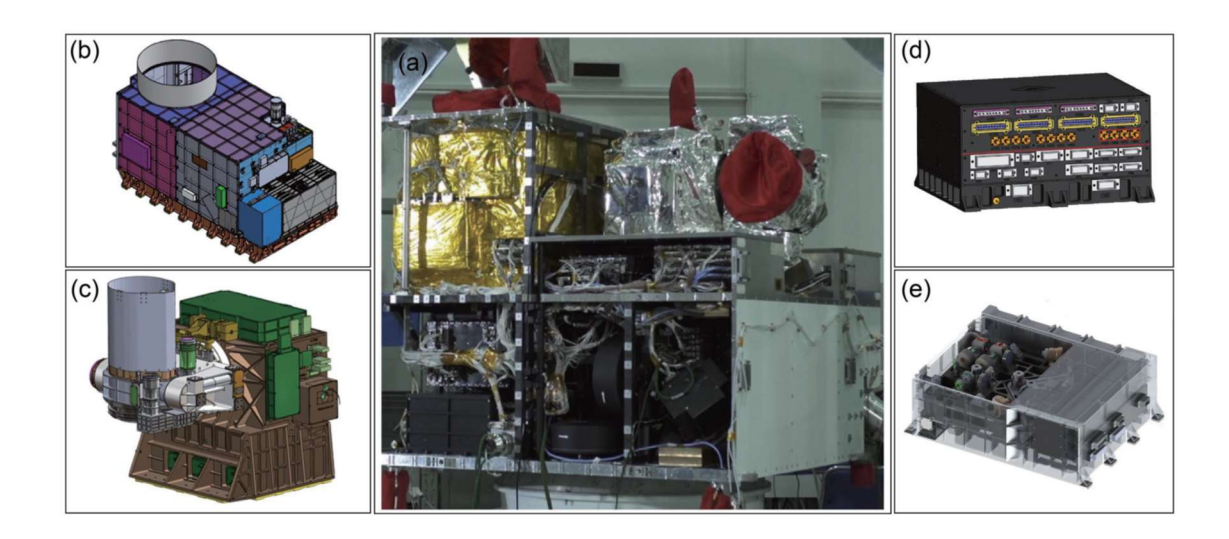
1.2.8. Conclusion on wavelength selection

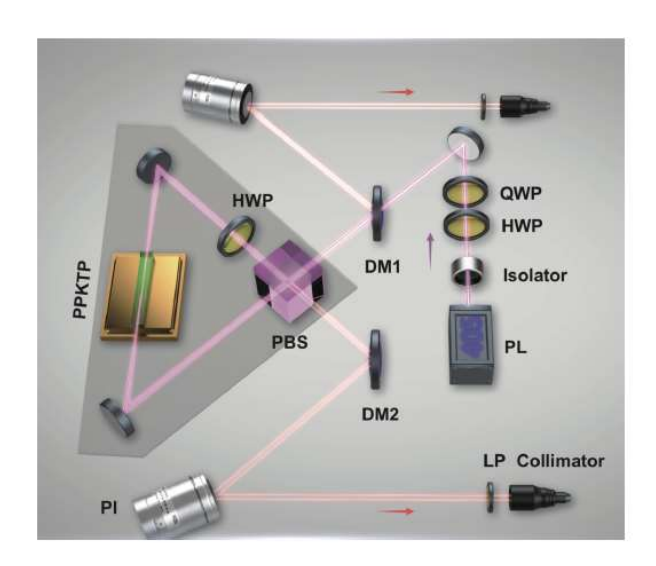
In light of the aforementioned factors, it can be concluded that a source producing SPDC photons between 750 nm and 850 nm represents the optimal choice for a flexible space-suitable source of entangled photons.

The experimental configuration for the production of entangled photon pairs via spontaneous parametric down-conversion is illustrated below. Type-II non-collinear phase matching in β -barium borate (BBO) is known to produce high-fidelity polarization entanglement. The additional birefringent crystals C1 and C2, in conjunction with the half-wave plate (HWP), serve to compensate for the birefringent walk-off effect within the crystal. A payload sketch has been proposed in [3] and depicted below.



Figures from [3]





2. Fundamental Concepts

2.1. Quantum state vector

The state of a quantum system is completely described by a state vector $|\psi\rangle$ embedded in a linear unitary vector space (Hilbert Space \mathcal{H}).

If two orthogonal vectors $|\psi_1\rangle$ and $|\psi_2\rangle$ ($\langle\psi_1\mid\psi_2\rangle=0$) are possible states of the quantum system then so is the coherent superposition state:

$$|\psi\rangle = \alpha |\psi_1\rangle + \beta |\psi_2\rangle$$

where $\alpha\alpha^* + \beta\beta^* = 1$ When a physical system can be described by means of a state vector, it is said to be in a pure state. This implies that the states $|\psi_1\rangle$ and

 $|\psi_2\rangle$ be decoupled from, i.e., identical in, any other degrees of freedom. Any correlations with uncontrolled external degrees of freedom reduce the purity of the superposition state.

States that cannot be described by state vectors are known as mixed states.

In this case there remains some uncertainty in the preparation procedure, and the physical system is described by means of a density operator.

2.2. Density matrix

The density operator describing a mixed state can be written as a sum of orthogonal projection operators $|\psi_i\rangle\langle\psi_i|$:

$$\hat{\rho} = \sum_{i} p_{i} |\psi_{i}\rangle\langle\psi_{i}|$$

Where $p_i > 0$ ($\sum_i p_i = 1$) is the probability with which the system resides in the pure state $|\psi_i\rangle$. For pure quantum state vectors, the density matrix reduces to the projection operator $|\psi_i\rangle\langle\psi_i|$, such that the relation $\hat{\rho}^2 = \hat{\rho}$ holds. In general, the degree of mixedness is quantified by the purity:

$$\mathcal{P}(\hat{\rho}) = Tr(\hat{\rho}^2)$$

The purity is one for a pure state and 1/N for a maximally mixed state of dimension N.

2.3. Quantum measurements

Assume an experimenter has an ensemble of identically prepared systems, each in a state $|\psi\rangle$ and performs a quantum measurement of an observable physical quantity on each system. In quantum theory, measurable quantities are described by means of **Hermitian operators** $\widehat{\mathcal{M}}$, whereby the operators' real eigenvalues correspond to possible measurement outcomes. Hermitian

operators can be decomposed in terms of orthogonal projection operators ($\widehat{\Pi}_i = |m_i\rangle\langle m_i|$):

$$\widehat{\mathcal{M}} = \sum_{i} m_{i} \widehat{\Pi}_{i}$$

These projection operators fulfil the relations:

$$\widehat{\Pi}_i^2 = \widehat{\Pi}_i$$

$$\widehat{\Pi}_i \widehat{\Pi}_j = \delta_{ij} \widehat{\Pi}_i$$

and can be considered as elementary observables that query the system, "are you in state $|m_i\rangle$. Their eigenvalues (1/0) can directly be interpreted as the response ("yes"/ "no") to such a query:

$$\widehat{\Pi}_i|m_i\rangle=\delta_{ij}|m_i\rangle$$

The probability of obtaining a measurement value m_i for a quantum system prepared in a state $|\psi\rangle$ is calculated as the expected value of the corresponding projection operator

$$P(m_i) = \langle \psi | \widehat{\Pi}_i | \psi \rangle = |\langle \psi | m_i \rangle|^2$$

After a quantum measurement has been performed, the state vector must be updated according to the random measurement outcome ml and the wave function "collapses" onto the eigenvector $|m_l\rangle$:

$$\frac{\widehat{\Pi}_l |\psi\rangle}{P(m_l)} = |m_l\rangle$$

When a quantum system is described by a density matrix $\hat{\rho}$, the probability of obtaining a measurement outcome m_i is calculated via the trace operator:

$$P(m_i) = \operatorname{Tr}(\hat{\rho}\widehat{\Pi}_i) = \sum_i \langle m_i | \hat{\rho}\widehat{\Pi}_i | m_i \rangle$$

Similarly, the expected value of the observable $\widehat{\mathcal{M}}$ is:

$$\langle \widehat{\mathcal{M}} \rangle = \operatorname{Tr} (\widehat{\rho} \widehat{\mathcal{M}})$$

2.4. Encoding Quantum Information in Photons

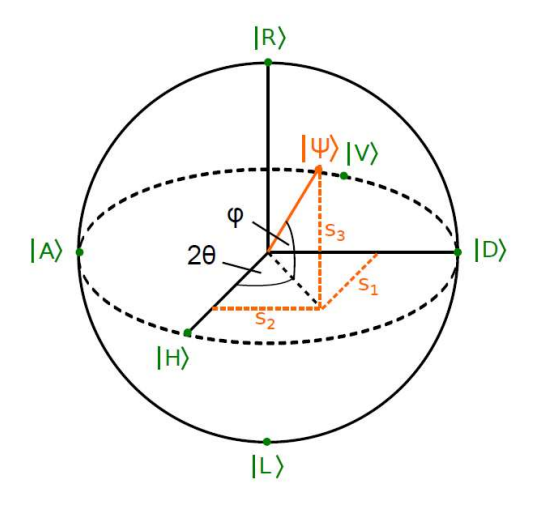
Two-dimensional quantum states, also known as qubits, can be encoded in a number of different degrees of freedom of photons [1]. The most common methods of encoding are time-bin and polarization encoding. Time-bin encoded qubits are predominantly employed in fibre-based quantum cryptography systems. Polarization qubits, however, are susceptible to polarization-mode dispersion in extended fibre optics, and the coherent transmission of such qubits via long fibre optic links is a more delicate matter. Nevertheless, polarization qubits have demonstrated exceptional suitability for transmitting quantum information over turbulent atmospheric free-space links, and have been employed in numerous fundamental tests of quantum theory at long distances. In the following sections, the focus will be on qubits encoded in the polarization states of single photons. For example: $|0\rangle \equiv |H\rangle$, $|1\rangle \equiv |V\rangle$

where $|H\rangle$ and $|V\rangle$ correspond to the vertical and horizontal linear polarization states.

2.5. Polarization states

A very useful way to visualize polarization states, is the geometrical representation on the Bloch's sphere (figures from [1]). In this representation, a pure state corresponds to a point on the surface of the sphere with polar coordinates 2θ and ϕ :

$$|\psi\rangle = \cos(\theta)|H\rangle + e^{i\phi}\sin(\theta)|V\rangle$$



The coordinate axes in figure above have been chosen as the eigenvectors of the Pauli operators:

$$\begin{split} \hat{\sigma}_1 &= |H\rangle\langle H| - |V\rangle\langle V| \\ \hat{\sigma}_2 &= |D\rangle\langle D| - |A\rangle\langle A| \\ \hat{\sigma}_3 &= |R\rangle\langle R| - |L\rangle\langle L| \end{split}$$

Together with the identity operator $\hat{\sigma}_0 = \mathbb{I}$, these operators form a complete basis for 2 × 2 Hermitian operators. Consequently, the density operator can be expressed as:

$$\hat{\rho}_s = \frac{1}{2}(\mathbb{I} + \boldsymbol{s} \cdot \widehat{\boldsymbol{\sigma}})$$

Where $\mathbf{s}=(s_1,s_2,s_3)$ is known as the Stokes vector and $\widehat{\boldsymbol{\sigma}}=(\widehat{\sigma}_1,\widehat{\sigma}_2,\widehat{\sigma}_3)$.

The elements of the Stokes vector are simply the expected values for polarization measurements in the Pauli basis $s_i = \operatorname{Tr}(\hat{\rho}(s)\hat{\sigma}_i)$. Stokes vectors representing pure states $|\Psi(s)\rangle\langle\Psi(s)|$ lie on the surface of the Bloch's sphere (|s|=1). The Stokes vectors lying inside the Bloch's sphere |s|<1 correspond to mixed states, with the centre of the sphere |s|=0 corresponding to the completely depolarized mixed state:

$$\hat{\rho}_{\text{unpol}} = \frac{1}{2} (|H\rangle\langle H| + |V\rangle\langle V|) \equiv \frac{\hat{1}}{2}.$$

polarization	state symbol	$ H\rangle, V\rangle$ decomposition	(s_1, s_2, s_3)
linear horizontal	$ H\rangle$	$ H\rangle$	(1,0,0)
linear vertical	$ V\rangle$	$ V\rangle$	(-1,0,0)
linear diagonal	$ D\rangle$	$\frac{1}{\sqrt{2}}\left(H\rangle+ V\rangle\right)$	(0, 1, 0)
linear antidiagonal	$ A\rangle$	$\frac{1}{\sqrt{2}}(H\rangle - V\rangle)$	(0, -1, 0)
right-handed circular	$ R\rangle$	$\frac{1}{\sqrt{2}}(H\rangle+i V\rangle)$	(0, 0, 1)
left-handed circular	$ L\rangle$	$\frac{1}{\sqrt{2}}(H\rangle - i V\rangle)$	(0,0,-1)

Table from [1]

2.6. Polarization measurement

A polarization measurement along a polarization direction n (|n| = 1) on the Bloch's sphere is described by the operator:

$$\hat{\sigma}_n \equiv \hat{\boldsymbol{\sigma}} \cdot \boldsymbol{n}$$

The state projectors corresponding to the measurement outcomes ($\sigma_n=\pm 1$) read:

$$\widehat{\Pi}(\sigma_n = \pm 1) = \frac{1}{2} (\widehat{1} \pm \widehat{\sigma}_n)$$

For a polarization measurement performed on a photon described by a Stokes vector s, the expected value of is given by:

$$\langle \hat{\sigma}_n \rangle = \operatorname{Tr} \left(\hat{\rho}(\boldsymbol{s}) \hat{\sigma}_n \right) = (\boldsymbol{s} \cdot \boldsymbol{n})$$

2.7. Polarization entanglement

In quantum theory composite quantum systems, comprising subsystems of two parties Alice (A) and Bob (B), are described by means of a state vector on the tensor product space $\mathcal{H}_A^2 \otimes \mathcal{H}_B^2$. A pure bi-partite quantum state that describes the composite system is called "entangled" if it cannot be written as a direct tensor product of individual state vectors of A and B $(|\psi\rangle_{AB} \neq |\psi\rangle_A \otimes |\phi\rangle_B)$. An important class of pure entangled states are the maximally entangled Bell states:

$$|\Psi^{\pm}\rangle_{AB} = \frac{1}{\sqrt{2}}(|H\rangle_{A}|V\rangle_{B} \pm |V\rangle_{A}|H\rangle_{B})$$
$$|\Phi^{\pm}\rangle_{AB} = \frac{1}{\sqrt{2}}(|H\rangle_{A}|H\rangle_{B} \pm |V\rangle_{A}|V\rangle_{B})$$

In a maximally entangled state, all information is shifted from the individual photons' polarizations to correlations between the polarizations of photons A and B. In order to see this let us assume Alice and Bob share a pair of photons in a $|\Phi^{\pm}\rangle_{AB}$ state and perform polarization measurements with linear polarizers

oriented at angles α and β , respectively. Inserting the projection operators for linear polarizers:

$$\widehat{\Pi}_{\alpha}^{A} = \frac{1}{2} (\widehat{1} + \cos(2\alpha)\widehat{\sigma}_{1} + \sin(2\alpha)\widehat{\sigma}_{2})$$

$$\widehat{\Pi}_{\beta}^{B} = \frac{1}{2} (\widehat{1} + \cos(2\beta)\widehat{\sigma}_{1} + \sin(2\beta)\widehat{\sigma}_{2})$$

the probability for a coincidence detection of two photons reads:

$$\langle \Phi^+ | \widehat{\Pi}_{\alpha}^A \otimes \widehat{\Pi}_{\beta}^B | \Phi^+ \rangle = \frac{1}{2} \cos^2 (\alpha - \beta)$$

This is a notable consequence of the fact that the relative orientation of the polarization analysers is the sole determining factor. Therefore, when a photon passes through Alice's polarizer, oriented at an angle α , she can state with certainty that Bob's photon will also pass through his polarizer, should he have chosen to orient his polarizer at the same angle. However, it is not possible for Alice to predict with certainty whether or not a given photon will pass her polarizer. This occurs with a probability of 50%. Therefore, while she is able to make definitive conditional predictions about the outcome of correlation measurements, she is unable to make any independent predictions about the polarization of her photon, given that it is dependent on the polarization of Bob's photon. More formally, when Alice attempts to describe the local state of her photon using a local density matrix $\hat{\rho}_A$, she does so by performing an average over Bob's possible measurement outcomes:

$$\hat{\rho}_A = \sum_{i=H,V} B\langle i|\hat{\rho}_{AB}|i\rangle_B = \operatorname{Tr}_B(\hat{\rho}_{AB})$$

with the partial trace operator Tr_B Bob's reduced polarization state is calculated analogously ($\hat{\rho}_B = \operatorname{Tr}_A(\hat{\rho}_{AB})$). When applied to a maximally entangled state, the partial trace yields a completely unpolarized mixed state.

It can be observed that, while the local measurement outcomes are entirely random, they can nevertheless be non-locally correlated. This intriguing

combination of non-local correlations and random local measurement outcomes led to the renowned Gedankenexperiment by Einstein, Podolsky, and Rosen, which subsequently became known as the EPR paradox.

2.8. Bell's inequality

In 1964 J. Bell showed that the assumption of underlying local realism leads to experimentally testable consequences. A modified version of his original argument goes as follows: Consider an experiment in which Alice and Bob can each perform one of two possible polarization measurements along the directions a, a' and b, b', respectively. If the two-valued measurement outcomes $(\sigma_a^A, \sigma_{a'}^A, \sigma_b^B, \sigma_{b'}^B = \pm 1)$ are pre-determined (local realism), then the following equation must hold:

$$S = (\sigma_a^A + \sigma_{a'}^A)\sigma_b^B + (\sigma_a^A - \sigma_{a'}^A)\sigma_{b'}^B = \pm 2$$

This also implies an upper bound for the expected value of $|\langle S \rangle|$

$$|\langle S \rangle| = \left| \langle \sigma_a^A \sigma_b^B \rangle + \left\langle \sigma_a^A \sigma_{b'}^B \right\rangle + \left\langle \sigma_{a'}^A \sigma_b^B \right\rangle - \left\langle \sigma_{a'}^A \sigma_{b'}^B \right\rangle \right| \le 2$$

Eq. is known as the CHSH (Clauser-Horne-Shimony-Holt) variant of Bell's inequality. Now let us calculate the quantum-mechanical prediction $\langle \hat{S} \rangle$

Assuming Alice and Bob share photon pairs in a maximally-entangled $|\Psi^-\rangle$ state, then the expected value for a joint polarization measurement is:

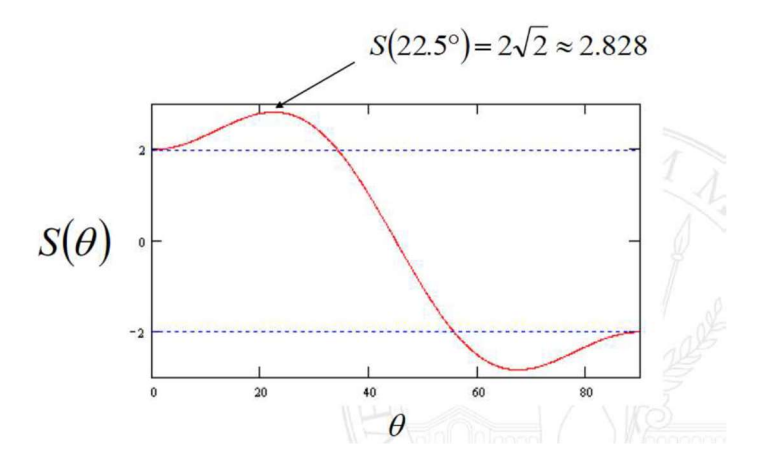
$$\left\langle \Psi^{-} \middle| \hat{\sigma}_{a}^{A} \hat{\sigma}_{b}^{B} \middle| \Psi^{-} \right\rangle = -\boldsymbol{a} \cdot \boldsymbol{b}$$

Now, considering, for example, polarization measurements along the directions $\mathbf{a}'=(1,0,0)$, $\mathbf{a}=(0,1,0)$, $\mathbf{b}=1/\sqrt{2}(1,1,0)$, $\mathbf{b}'=1/\sqrt{2}(-1,1,0)$ on the Bloch's sphere the quantum-mechanical expected values are:

$$\langle \hat{\sigma}_{a}^{A} \hat{\sigma}_{b}^{B} \rangle = \langle \hat{\sigma}_{a}^{A} \hat{\sigma}_{b'}^{B} \rangle = \langle \hat{\sigma}_{a'}^{A} \hat{\sigma}_{b}^{B} \rangle = -\frac{1}{\sqrt{2}}$$
$$\langle \hat{\sigma}_{a'}^{A} \hat{\sigma}_{b'}^{B} \rangle = \frac{1}{\sqrt{2}}$$

We thus see that quantum mechanics predicts a violation of the CHSH inequality:

$$\langle \hat{S} \rangle = \frac{4}{\sqrt{2}} = 2\sqrt{2} \approx 2.828 > 2$$



The violation of Bell's inequality has been verified in numerous Bell test experiments with entangled particles, which irrefutably demonstrate that a local realistic interpretation of quantum entanglement cannot hold.

2.9. Bell-state fidelity

In a laboratory setup, experimental imperfections inadvertently lead to some degree of impurity in the preparation of entangled qubits. A common way of quantifying the quality of the prepared state $\hat{\rho}$ is its overlap fidelity with an ideal target state.

In the case of a pure target state, e.g., the maximally entangled Bell state $|\Psi^{-}\rangle$, the fidelity is defined as:

$$F_{\Psi^{-}}(\hat{\rho}) = \operatorname{Tr}(\hat{\rho}|\Psi^{-}\rangle\langle\Psi^{-}|)$$

When the generated state has perfect overlap with the ideal Bell state, the fidelity is 1, and for a completely mixed state the fidelity is 0.25. Typically, entanglement is ensured when F>0.5. The overlap fidelity is computed by reconstruction of the density matrix via quantum state tomography.

Quantum state tomography is a procedure for reconstructing the density matrix of an unknown quantum state from a set of measurements performed on an ensemble of identically prepared particles. To see how

this can be accomplished for polarization-entangled photon pairs, consider the general definition of a two-qubit density matrix in terms of the complete set of Pauli matrices:

$$\hat{\rho} = \frac{1}{4} \Big(\sum S_{ml} \hat{\sigma}_m \otimes \hat{\sigma}_l \Big)$$

The coefficients \mathcal{S}_{ml} can be interpreted as two-photon Stokes parameters:

$$S_{ml} = \operatorname{Tr}\left(\hat{\rho}(\hat{\sigma}_m \otimes \hat{\sigma}_l)\right)$$

The two-photon Stokes parameters, and thus the density matrix of the two photons, can be reconstructed by performing $6\times6=36$ elementary projective measurements $|i\rangle\langle i|_A |j\rangle\langle j|_B$ where i,j=H,V,D,A,L,R)

3. Quantum Positioning System

In order to overcome the inherent limitations of accuracy associated with energy and bandwidth in classical measurement processes and to further enhance the confidentiality of current navigation and positioning systems, a quantum positioning system (QPS) based on quantum measurement technology has been proposed. The QPS employs the quantum entanglement and squeezing properties, thereby enabling the transmitted quantum information to gain strong correlation and high density. This, in turn, allows for the provision of long-term and high-accuracy positioning services. In fact, the position of Alice can be determined by transmitting pulses from her position and measuring the time taken for each pulse to reach the reference points. The position of the subject is determined by three factors: the time of flight of the pulses, the speed of the pulses and the arrangement of the reference points. The degree of accuracy achievable by this method is contingent upon the number of pulses employed, the bandwidth of these pulses and the number of photons per pulse. By measuring the correlations between the times of arrival of M pulses that are frequency-entangled, it is possible to increase the accuracy of such a positioning procedure by a factor of \sqrt{M} in comparison to positioning using

unentangled pulses with the same bandwidth. Furthermore, the generation of number-squeezed pulses allows for an additional enhancement of \sqrt{N} through the employment of squeezed pulses with N quanta, as opposed to the utilization of "classical" coherent states with N quanta. The combination of entanglement and squeezing results in an overall improvement of \sqrt{MN} . Furthermore, the procedure exhibits enhanced security, as the timing information is embedded within the entanglement between pulses. This enables the implementation of quantum cryptographic schemes that prevent an eavesdropper from acquiring information about Alice's position. However, the primary challenges associated with this approach are the difficulty in establishing the necessary entanglement and the susceptibility to loss. Conversely, frequency entanglement provides a means to construct highly resilient schemes against pulse broadening caused by transmission through dispersive media. Concurrently, the robust security of quantum mechanics enables the development of a highly confidential positioning system. The use of second-order coherence in entangled photons in the time domain enables the QPS to achieve a significantly enhanced level of measurement precision, approaching the physical limit set by the Heisenberg uncertainty principle, in comparison to that of a classical positioning system. It can be utilized for the navigation and positioning of stationary or moving targets, as well as for the determination of relative orbits in low Earth orbit, deep space and interplanetary spacecraft, and so forth. As a nascent technology, the viability and efficacy of quantum navigation and positioning technology have been demonstrated. Nevertheless, the advancement of research in this field has been gradual since the concept and model of QPS were first proposed in 2001. This can be attributed to several factors: (1) The functioning of QPS is contingent upon the transmission and reception of quantum entangled photon pairs. The preparation of long entanglement, high-quality and power entangled signals represents a nascent technology that is being continually explored. (2) Once the quantum-entangled signals have been prepared, it is necessary to have the appropriate devices in place for processing, manipulating and storing the quantum signal. Given that the entanglement characteristics are susceptible to external influences, it is imperative to conduct further research into the

preservation of quantum signal purity. (3) The quantum signals in question are often extremely weak, necessitating the use of detectors with enhanced efficiency and sensitivity to ensure accurate detection.

It may be the case that the performance of classical detectors does not meet the requisite standards, necessitating the development of a high-performance single-photon detector.

A positioning system can be classified as either passive or active, depending on whether it engages with the external environment. A passive positioning system employs quantum sensor devices to achieve attitude adjustment and positioning, obviating the necessity for real-time signals from on-orbit satellites for ranging and timing. As previously outlined in Chapter 1, an illustrative example of this technology is the atomic interferometer gyroscope, which is based on the Sagnac effect. The fundamental principle underlying the atomic interferometer gyroscope is the movement of cold atoms in opposing directions along a shared parabolic trajectory, which gives rise to the formation of an atomic beam. This beam is then subjected to an interference loop under the influence of a Raman laser. Given that the phase shift difference of the doubleloop interference is contingent upon the rotation rate, it is possible to extract further information regarding angular velocity. The theoretical value of drift is considerably lower than that of a classical gyroscope. Similarly, the atom accelerometer is also based on the Sagnac effect of the atom, and thus its development trajectory is almost identical to that of the atomic interferometer gyroscope. In addition to the interferometer gyroscope, the angular velocity can be sensed by utilizing the spin of alkali metal atoms, based on the Larmor precession rate of an atom. Such a device is referred to as an atomic spin gyroscope.

Active QPS is founded upon the principles of quantum measurement. The system employs frequency-entangled quantum pulses as the information carrier, utilizing the time difference of arrival (TDOA) between entangled photon pairs to determine the user's position. In the context of quantum navigation and positioning, it is necessary to conduct quantum ranging based on the principle of optical interference, whereby the second-order correlation between the signal

light and the idle light in the entangled two-photon pair is measured. It can provide super-resolution of the distance, which is much below the Rayleigh diffraction limit. In comparison with a classical global positioning system based on electromagnetic waves, active QPS can obtain higher positioning accuracy and better confidentiality.

This work mainly discusses the current research status and prospects of active QPS and its key components.

3.1. Quantum entanglement preparation technology

The entanglement of transmitted photons plays a significant role in the quantum navigation and positioning system [4]. In order to implement a quantum-based ranging process, it is necessary to generate entangled states and prepare quantum entanglement, which is a prerequisite for QPS. There are multiple techniques for generating entangled states, including the spontaneous parametric down-conversion (SPDC) process in a nonlinear crystal, the ion trap method, and the cavity quantum electrodynamics (C-QED) approach. The technology for preparing entangled states is evolving towards more straightforward implementation, higher entanglement purity, and the ability to generate multi-body or multi-degree of freedom states. The aforementioned preparation methods will be discussed in further detail in this section.

3.1.1. Preparation of photon entangled states by SPDC

Among the various methods of entangled state generation, the SPDC method is the most versatile and efficient. This process involves the spontaneous splitting of a pump photon into a pair of lower energy photons due to second-order nonlinear interactions. The experimental setup for the SPDC process is illustrated in the figure below.

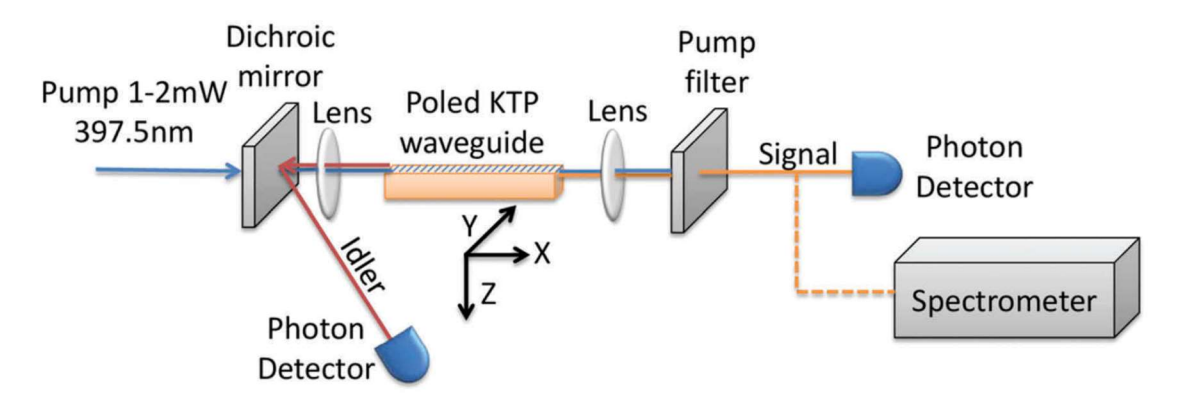


Figure from [4]

When a beam of pump light is incident upon a nonlinear crystal, the photon will split randomly according to a certain probability, thereby generating entangled signal light and idle light. This process is in accordance with the conservation of energy and momentum, which can be expressed as follows:

$$\omega_p = \omega_i + \omega_s$$
$$\mathbf{k}_p = \mathbf{k}_i + \mathbf{k}_s$$

where ω_p , ω_i and ω_s are frequencies of pump light, idle light and signal light photon, respectively; \mathbf{k}_p , \mathbf{k}_i and \mathbf{k}_s are the corresponding light wave vectors. The entangled photon pairs generated by SPDC can be entangled in a number of different ways, including in terms of momentum, frequency, time-energy and polarization.

In 1990, Rarity and Tapster conducted an experiment to prepare a momentum-entangled state of two photons. With regard to the preparation of energy-time entanglement, Franson demonstrated that a further form of non-local interference could be generated by the use of two particles emitted simultaneously in 1989. Subsequently, Brendel and Kwiat et al. conducted an experiment to validate the theoretical proposal, thereby confirming the existence of this particular form of entanglement. This type of entanglement has a physical interpretation whereby the coincidence count obtained at different times corresponds to the different paths of the two photons. Consequently, this entanglement state is subsequently referred to as energy-time entanglement. With regard to the preparation of polarization entanglement, this was achieved at an early stage through type-I SPDC. However, this scheme necessitates the

use of additional optical components, as well as a post-selection process that aligns with the detector. Consequently, the preparation efficiency is relatively low. An alternative, more convenient method for generating polarized entangled two-photon states is through type-II parametric down-conversion, which obviates the need for additional optical devices to generate entangled photons. The image of the SPDC spatial profile type-II light field is shown in the figure below.

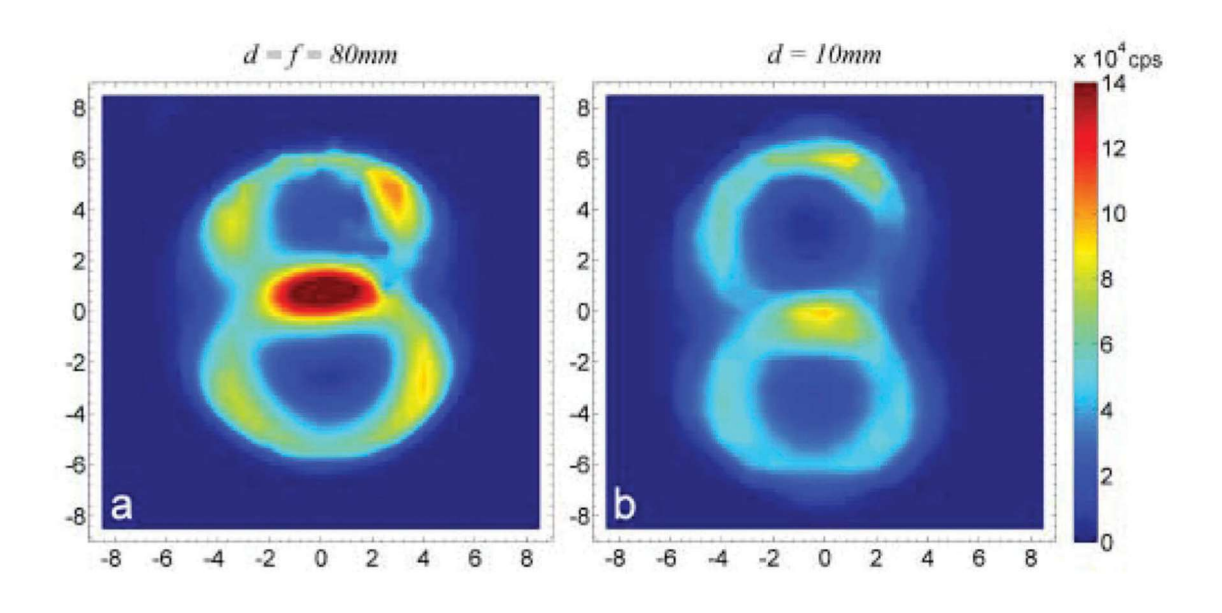


Figure from [4]

In 1999, Kwiat proposed a novel method for generating polarized entangled photon pairs. This involved the use of two type-I nonlinear phase-matching crystals, with their optical axes positioned in two perpendicular planes. Upon interaction with a polarized pump beam of light, each crystal produced a pair of entangled photons. A significant benefit of this approach is that the non-maximum entangled state can be readily generated by modifying the polarization state of the pump light. Furthermore, the brightness and purity of the entanglement source prepared by this method are significantly enhanced in comparison to the previous method. The entangled photon pairs prepared by the aforementioned method are entangled in multiple degrees of freedom. Consequently, Barreiro put forth a methodology for the preparation of a

hyperentangled state through the implementation of suitable extraction operations. The hyperentangled state is of significance for a number of applications, including quantum positioning, error correction coding, and the overcoming of channel noise in quantum communication. Additionally, it has potential applications in the field of quantum computing.

The preparation of an entangled state using SPDC has become a topic of considerable interest within the field of quantum information science. New experimental schemes have been proposed on a regular basis, and the efficiency, purity and convenience of entanglement sources have been enhanced. In 1998, Keller put forth a methodology for the preparation of a maximally entangled state of three photons. In the same year, Bouwmeester observed the polarization entanglement of three spatially separated photons for the first time experimentally, utilizing two pairs of entangled photons based on linear optics. In 1999, Ou and Lu employed cavity-enhanced SPDC to reduce the bandwidth of the entangled photon pair, thereby facilitating the detection of the entangled photon pair. Consequently, the number of entangled photon pairs received per unit time was increased to a certain extent. In 2000, Sanaka put forth a methodology for the preparation of entangled photon pairs utilizing a Concurrently, Tanzilli employed waveguide-type nonlinear device. comparable approach to generate entangled photon pairs. In contrast to the preceding methodologies, which are based on birefringent phase matching (BPM), this approach employs a technique known as quasi-phase matching (QPM). This has the effect of enhancing the brightness of the entanglement source by four orders of magnitude in comparison to the previous method utilizing BPM. In 2001, Kurtsiefer optimized the collection scheme of entangled photon pairs, thereby enhancing the generation efficiency of entanglement sources. This technology was employed to collect a total of 360,000 entangled photon pairs per second in the near infrared region of single-mode fibre. In 2003, Zhao successfully prepared the four-photon Greenberger-Horne-Zeilinger (GHZ) state in experiments, and in the following year, Pan and his team successfully prepared the five-photon entangled state, which they used to demonstrate the teleportation of a quantum state with open terminals. The

results, published in Nature that year, were among the top ten advances of the year as recognized by both the European and American Physical Societies. In 2006, the teleportation of a quantum state comprising two particles was achieved, as was the successful preparation and manipulation of a six-photon entangled state for the first time in an experiment. These results were featured on the October 2006 cover of Nature Physics. In 2011, Guo's team successfully prepared eight photon entangled states. In 2018, Zhong designed and realized the entanglement of 12 photons by using the SPDC method, achieving a state fidelity of 0.572 ± 0.024. The experimental setup is shown in the figure below.

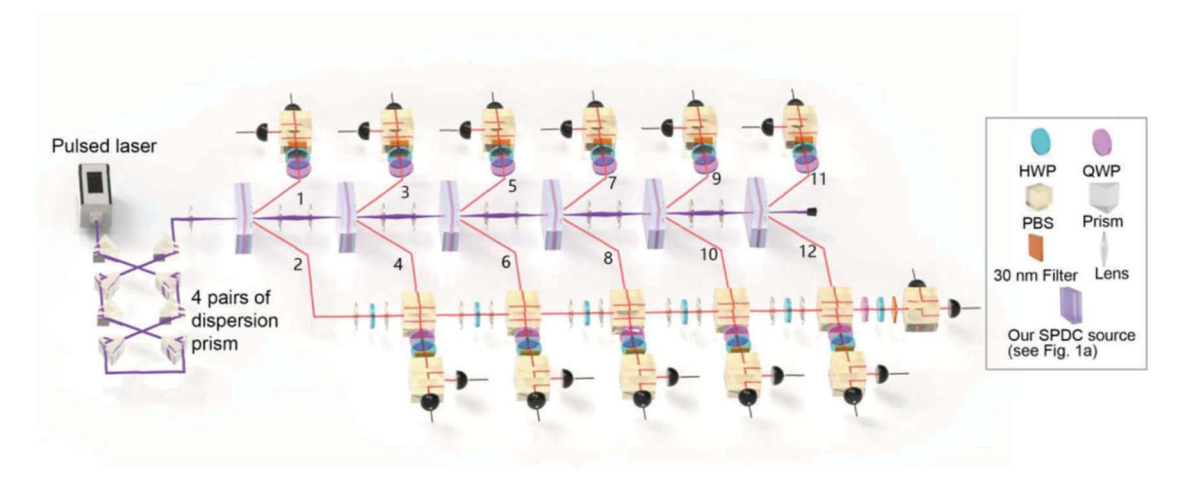


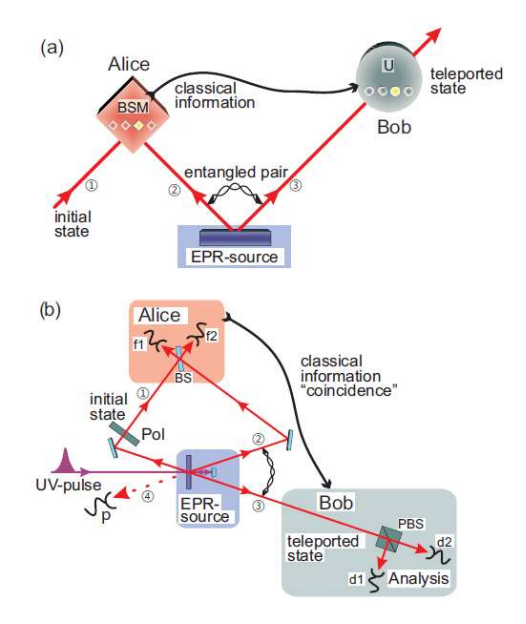
Figure from [4]

In the context of maximum quantum entanglement state preparation, Philip et al. conducted an analysis of the process of generating entangled photon pairs through SPDC in a quadratic nonlinear asymmetric waveguide coupler. They employed coupled mode hybridization and dispersion to alter the balance between the group velocities of the interacting pump, signal and idle light field. This resulted in a notable enhancement in the spectral factor (purity) of the generated photons. Giese investigated the impact of pump coherence on SPDC. In 2016, Frank conducted an experiment utilizing SPDC in a lithium niobate micro-disk resonator to generate entangled photon pairs, thereby demonstrating the realization of the SPDC process at a low power and microscale.

3.2. Space optical communication and quantum satellite system

The distribution of entangled photon pairs represents a fundamental aspect of quantum-related applications. In a large-scale quantum communication scheme, it is necessary to address the issues of energy loss, changes in polarization characteristics and decoherence in the transmission channel as the distance between the sender and receiver increases. The use of a terrestrial free space channel will result in the absorption of photon energy by the atmosphere, leading to attenuation. Furthermore, the maintenance of the link will be influenced by atmospheric conditions or ground obstructions. Consequently, single photons are only capable of traversing a restricted distance through silicon fibres or free space on land, thereby rendering the implementation of large-scale quantum communication unfeasible. Presently, the satellite communication technology, which is currently in widespread use, offers a potential solution for global quantum teleportation. This technology can overcome the distance limitation in optical fibre and land free-space links, thereby greatly extending the range of quantum teleportation and enabling the distribution of quantum entangled photon pairs on a large scale.

Quantum teleportation (Bennett et al., 1993) represents a means of faithfully transferring quantum states. The process of quantum teleportation relies on the utilization of both a classical channel and a quantum channel entanglement, which are shared between the two communication parties (see fig. below from [4]).



The quantum state to be **teleported**, for example, can be the polarization of a single photon, which can be written as: $|\chi\rangle_1 = \alpha |H\rangle_1 + \beta |V\rangle_1$, where α and β are two unknown, complex numbers satisfying $|\alpha|^2 + |\beta|^2 = 1$ and $|H\rangle_1$ and $|V\rangle_1$ denote the horizontal and vertical polarization states, respectively, which can be used to encode the basic logic 0 and 1 for a qubit. The entangled state of a pair of photons can be written as $|\phi^-\rangle_{23} = (|H\rangle_2 |H\rangle_3 - |V\rangle_2 |V\rangle_3)/\sqrt{2}$ one of the four maximally entangled two-qubit Bell states. Alice performs a joint measurement on the to-be-teleported photon 1 and the photon 2 from the entangled pair, projecting them into one of the four Bell states. Then the joint three-photon system is in the product state

$$|\psi\rangle_{123} = |\chi\rangle_1 \otimes |\phi^-\rangle_{23}$$

which can be decomposed into:

$$|\psi\rangle_{123} = \frac{1}{2} \begin{bmatrix} -|\psi^{-}\rangle_{12}(\alpha|H\rangle_{3} + \beta|V\rangle_{3}) - |\psi^{+}\rangle_{12}(\alpha|H\rangle_{3} \\ -\beta|V\rangle_{3}) + |\phi^{-}\rangle_{12}(\alpha|V\rangle_{3} + \beta|H\rangle_{3}) \\ + |\phi^{+}\rangle_{12}(\alpha|V\rangle_{3} - \beta|H\rangle_{3}) \end{bmatrix}$$

Subsequently, Bob is apprised of the result of the Bell-state measurement (BSM) through the medium of classical communication. In light of this information, he proceeds to implement a Pauli correction on photon 3. It is important to note that quantum teleportation does not violate the no-cloning

theorem. Following the successful teleportation of photon 1, the original state of photon 1 is no longer available, and thus photon 3 is not a clone, but rather the result of teleportation. Moreover, the quantum state can only be recovered once Bob has received the classical information sent by Alice. In accordance with the principles of relativity, the velocity of the transmission of classical information is constrained to a value no greater than that of light. Therefore, superluminal communication cannot occur as a consequence of quantum teleportation.

The space quantum communication scheme can be divided into two categories, ground-based and space-based, depending on the sender of the single photon (entangled photon pair).

The ground-based scheme comprises a ground-based transmitter terminal that is capable of distributing single photons to ground stations and satellites, or of sharing entangled photons. This allows for the implementation of quantum teleportation between disparate terminals. In the most basic scenario, a ground terminal can establish a direct communication link with another via a terrestrial free space link. However, the communication range in this configuration is constrained. In the space-based scheme, the light source (either a single photon or an entangled photon pair) is situated on the space transmitting platform, with the optical communication link traversing either the satellite-underground channel or the intersatellite channel. The satellite-underground optical link is less susceptible to atmospheric turbulence, whereas the satellite-to-satellite optical link is largely unaffected. Consequently, this communication scheme is well-suited to establishing longer links, which is also a global quantum teleportation scheme that is more readily implementable.

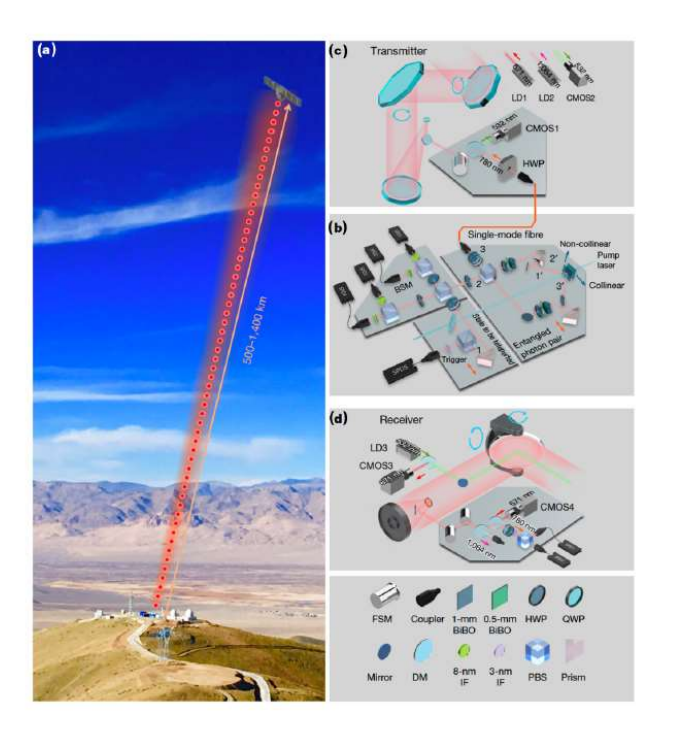


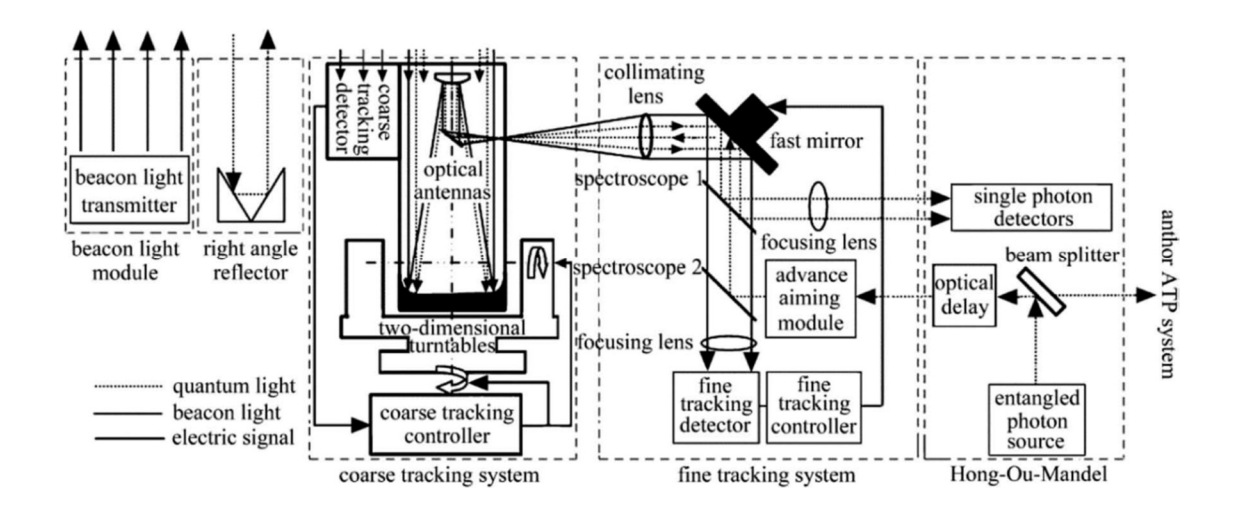
Figure from [3]. Overview of the set-up for ground-to-satellite quantum teleportation of a single photon over distances of up to 1,400 km.

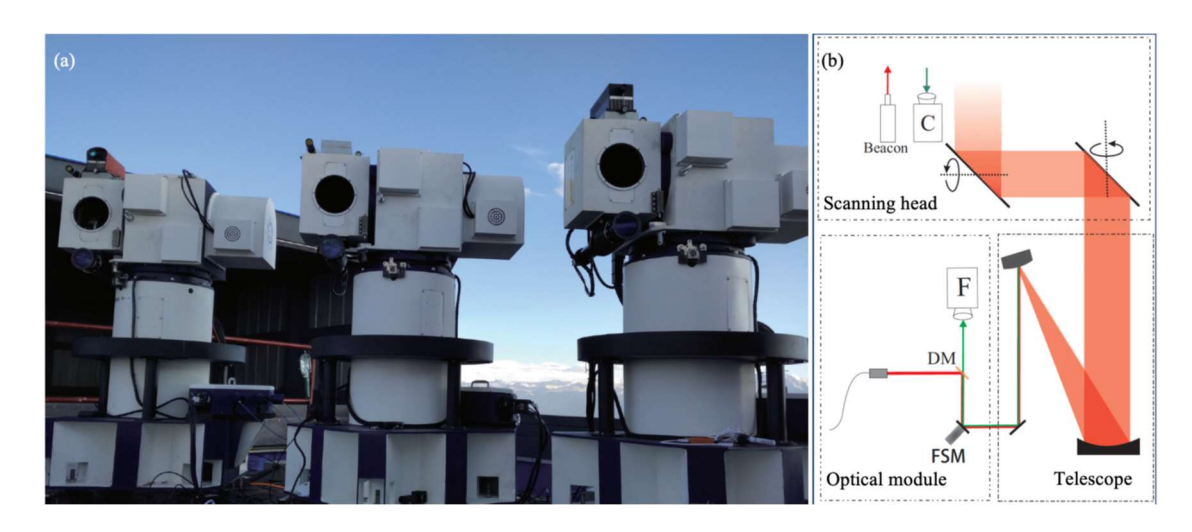
The advent of space optical communication can be traced back to the invention of the laser in the 1960s.

In 1970, Nilo Lindgren highlighted the issue of loss in optical fibre communication and indicated that NASA would deploy two synchronous satellites for inter-satellite and satellite-earth optical communication experiments in 1973 and 1974. From the 1980s to the 1990s, numerous countries proposed their own spatial optical communication strategies, developed ground test platforms, and initiated the construction of optical ground stations. However, it should be noted that spatial optical communication also has certain disadvantages. (1) Due to the small divergence angle and strong directivity of the laser, spatial optical communication relies on the acquisition, tracking and targeting subsystem to achieve and maintain high-precision optical alignment; (2) when a laser propagates in the atmosphere, it is susceptible to disturbance. (3) Point-to-point transmission features enhance the security of spatial optical communication, but also make it difficult to cover a large area in

network applications; (4) Remote communication makes it challenging to track and detect weak light.

Furthermore, atmospheric attenuation, turbulence and other effects present additional challenges.





Figures from [4] (upper) and [3] (below)

In 1985, the European Space Agency (ESA) spearheaded research on spaceearth and inter-satellite laser communication in Europe. In 2004, the University of Vienna proposed the Space-QUEST plan to ESA, which aimed to test freespace quantum communication between satellites and ground users. The satellite terminals were designed with the capability of establishing communication links with two ground stations and achieving the entangled photon pair distribution to both simultaneously. In order to facilitate the independent acquisition and tracking of the two ground station terminals, it is necessary to implement two acquisitions, tracking and pointing (ATP) systems for the satellite-based quantum communication terminals. The project is still in progress. Moreover, the SILEX project led to the development of the secondgeneration Laser Communication Terminal (LCT) in Germany, which employs BPSK modulation and detection. In 2008, the TerraSAR-X satellite, which was with the second-generation LCT, successfully established intersatellite laser communication with the U.S. near-field infrared experiment (NFIRE) satellite. The data rate achieved was 5.6 Gbps, and the communication distance was 6,000 km. In the 1980s, Japan initiated two significant projects: the ETS-VI and OICETS. The ETS-VI project enabled Japan to successfully implement satellite and ground laser communication between the ETS-VI satellite terminal and the ground station, with a data rate of 1.024 Mbps. In the OICETS project, the data communication rate between the OICETS satellite and the ESA's ARTEMIS was 50 Mbps.

In 1996, the optical communication terminal carried by Japan's high-orbit satellite ETS-VI and the ground station of the U.S. Jet Propulsion Laboratory (JPL) established a two-way laser link, thereby completing the world's first high-orbit satellite-Earth laser communication. Consequently, an on-orbit experiment in optical communication was initiated. Subsequently, free space optical communication has undergone a period of accelerated development, with numerous in-orbit experiments conducted between the mid-1990s and the early twenty-first century. Furthermore, the OICETS project conducted inter-satellite optical communication experiments with the ESA's ARTEMIS satellite, with a communication distance of over 36,000 km. This was done to verify the tracking technology, optical communication technology and space environment adaptability of devices for inter-satellite laser communication.

In 1995, the U.S. Ballistic Missile Defence Organization (BMDO) initiated the STRV-2 study of the satellite-Earth optical communication program, with the principal objective of establishing a bidirectional communication link between the low-orbit satellite TSX-5 and the ground station.

In 2008, NASA initiated the development of the Lunar Atmosphere and Dust Environment Explorer (LADEE). Given the satellite's additional capacity to accommodate additional payloads, NASA opted to utilize this opportunity to conduct a lunar laser communication demonstration (LLCD). The LADEE mission was launched in September 2013. The laser communication terminal on board the spacecraft subsequently made history by establishing a data transmission link between the Moon and Earth of approximately 400,000 km, with a record-breaking download rate of 622 Mbps and an upload rate of 20 Mbps. The onboard terminal of the LLCD project, designated LLST, comprises an optical module, a modulation module, and a control module.

In terms of equipment miniaturization, Takenaka and his team conducted an experiment utilizing a 48 kg low Earth orbit microsatellite to facilitate finite quantum communication with the ground. This is a notable achievement in the miniaturization and cost-effectiveness of space-based quantum experiment equipment. In China, the University of Electronic Science and Technology of China initiated research on free-space optical communication in the 1970s and subsequently developed and demonstrated an optical communication system between satellites. In 2011, the optical communication terminal developed by the Harbin Institute of Technology was carried on the LEO satellite Ocean-II, thereby establishing a satellite ground optical communication link. The uplink transmission rate was 20 Mbps, while the downlink was 504 Mbps, and the average capture time of the satellite was less than 5 s. The quantum satellite system is based on free-space quantum teleportation technology. In 2003, Pan and his team were the first to undertake experimental research on long-distance free-space quantum teleportation.

By the end of 2004, the team had successfully demonstrated the distribution and distribution of quantum keys in a free space of 13 km, thereby proving that the quantum properties of the photon entangled state could remain effectively after penetrating the atmosphere. This achievement constituted the first verification of the feasibility of satellite-earth quantum communication. Subsequently, Pan and his team conducted a series of ground verification experiments, including 16 km and 100 km free space quantum teleportation and

comprehensive ground verification of satellite ground quantum communication. These experiments have established a robust scientific and technical foundation for the realization of satellite-earth quantum teleportation.

In 2016, China launched the world's first quantum satellite, designated 'Mozi', and achieved the first quantum communication between a satellite and a ground station. The satellite has a mass of 640 kg and is designed to operate in a sunsynchronous orbit with an orbital inclination of 97.37 degrees. Its operational lifespan is estimated to be two years. China has successfully conducted experiments on high-speed quantum key distribution between satellite and ground station, long-distance free-space quantum key distribution during the daytime, and intercontinental quantum network establishment in satellite relay. The successful development and launch of the 'Mozi quantum satellite' has enabled China to establish a leading position in the field of quantum communication.

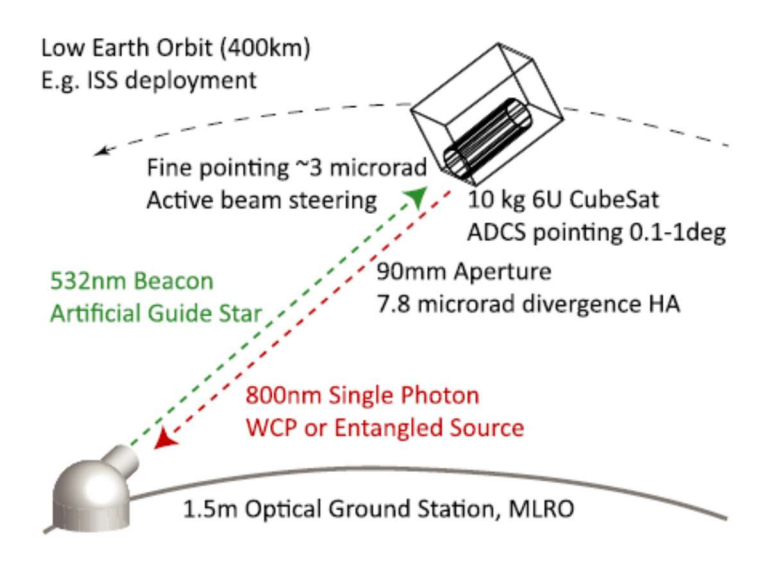
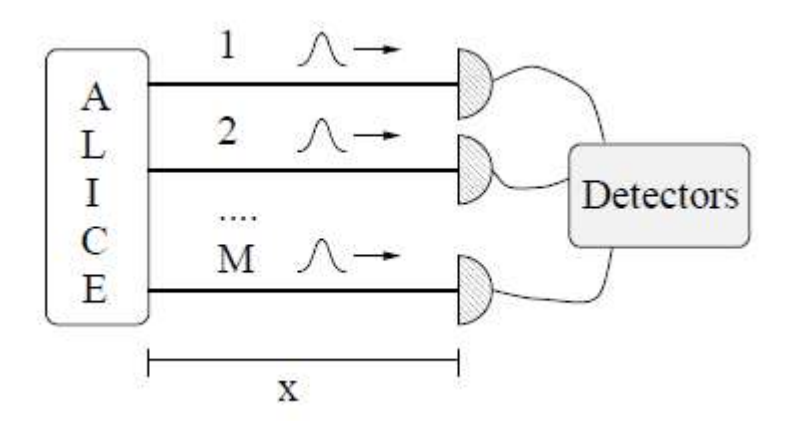


Figure from [7]. The CQuCoM 6U CubeSat deployed from the ISS into a circular low-Earth orbit. The ground track includes the Matera Laser Range finding Observatory

4. Research status of quantum positioning and quantum clock synchronization technology

The QPS is based on quantum-enhanced measurement technology and no longer utilizes electromagnetic waves, thereby conferring advantages in terms of accuracy, confidentiality and anti-interference capability. The concept of QPS was initially proposed by Dr. Giovannetti of the Massachusetts Institute of Technology (MIT) in 2001. Subsequently, it was demonstrated that the quantum entanglement and compression properties could enhance the precision of ranging and positioning. The principle of the ranging process based on quantum interferometry is illustrated in figure below.



By transmitting M entangled light pulses and calculating the meantime taken for these M pulses to reach the detector, the emitter, Alice, can obtain her positional information with an enhanced measurement accuracy of \sqrt{M} times. If each pulse contains N photons, the measurement accuracy can be enhanced to \sqrt{M} N times. In practical applications, the arrival of entangled photon pairs at detectors along different paths allows for the acquisition of TDOA values with picosecond accuracy through the use of second-order quantum coherence, thereby enabling the measurement of distances with a micron-level precision that is significantly superior to that achievable through classical radio-based positioning methods.

In 2002, Giovannetti put forth the concept of quantum-encrypted positioning and examined two protocols for quantum encryption, which bear resemblance to the

BB84 protocol for quantum key distribution. Concurrently, he devised and validated the 'conveyor belt clock synchronization' scheme, which is based on a synchronous desorbed quantum clock. This demonstrated that the synchronization of the clock is immune to the interference of a dispersed medium under typical circumstances, where quantum photons may potentially propagate. Consequently, this enhanced the precision of quantum positioning. In 2004, he provided further insight into how quantum-enhanced measurements surpass the limitations of conventional techniques. In 2008, Villoresi et al. advanced the concept of QPS by demonstrating the feasibility of teleportation of quantum signals between free space and Earth. In 2018, Luca Calderaro et al. conducted a study on the feasibility of space quantum communication experiments in high Earth orbit. Their investigation focused on the 20,000 km single photon teleportation experiment, which was based on the global positioning system. In 2019, Costantino Agnesi et al. also conducted experiments on the transmission of photon pulses by medium-Earth orbit satellites, achieving a measurement accuracy of 230 picoseconds at a distance scale of 7,500 km.

In 2004, Dr. Bahder of the U.S. Army Research Laboratory put forth the concept of the interferometric quantum positioning system (QPS) [5]. The QPS he proposed can be constructed according to different design specifications, one of which comprises three baseline pairs of six satellites, the spatial coordinates of which are known. The positioning principle is based on the time difference of arrival (TDOA). Two photons exhibiting frequency entanglement characteristics are positioned at a specific point along the baseline and transmitted to two satellites on the baseline, respectively, with the objective of measuring the time difference of arrival (TDOA) between two reference points. The three-dimensional position coordinate of the user can be calculated using the three TDOA values. The addition of an additional baseline allows for the determination of the space-time coordinate of the user. In this configuration, the user is required to have a three-sided angular reflector, a stable clock, and a classical channel for two-way communication with the reference position. In order to obtain the user's four-dimensional space-time coordinates (t, x, y, z), four

interferometers are required to receive four entangled pairs from satellites. Of these, three are employed to determine the user's spatial position, while the fourth is used to synchronize the user's clock with the reference position clock. A schematic diagram of the aforementioned scheme is provided in the figure below.

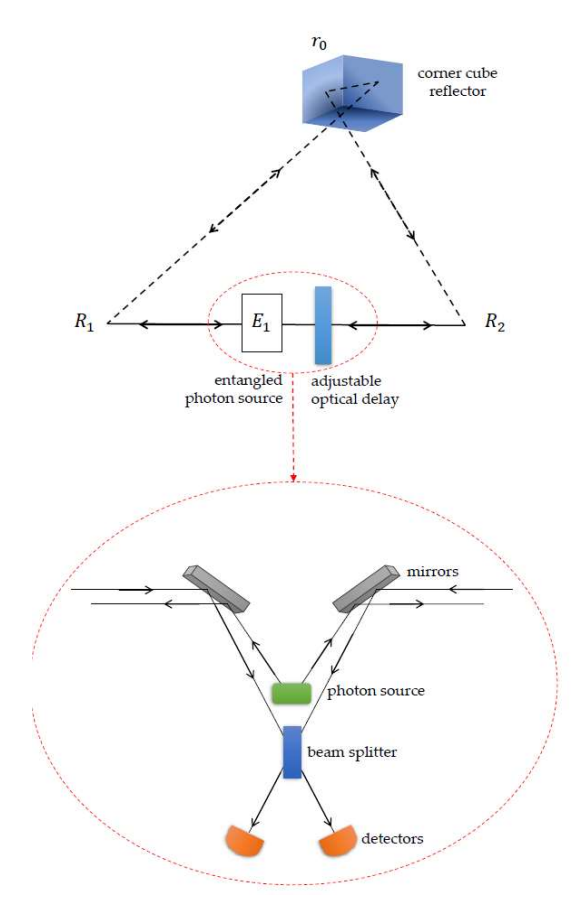
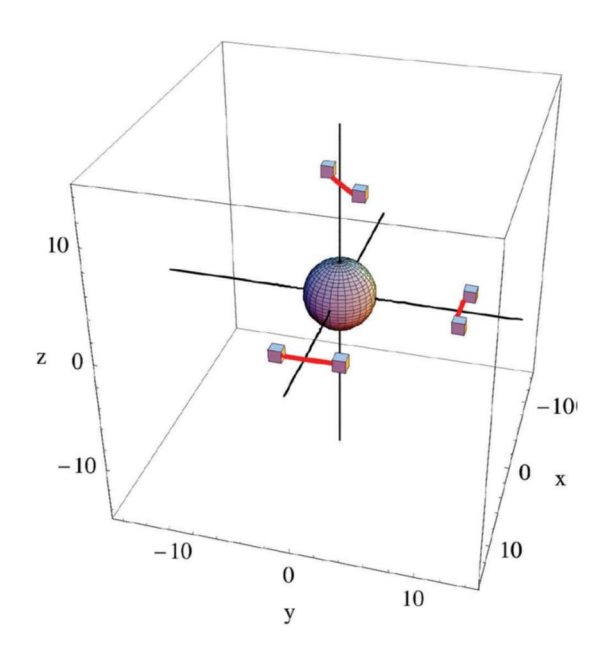


Figure from [5]

An alternative configuration involves the installation of a 50:50 beam splitter, single-photon detector, coincidence counter and optical delay unit at the ground user's location. The user is responsible for controlling the optical delay unit and for obtaining the coordinates of each baseline endpoint from the classical channel. Additionally, the user can determine the position of each endpoint through the application of the equations derived from the three TDOA values. The fundamental premise of QPS, as illustrated in reference [6], is based on the concept of a baseline.

$$t_L = \frac{2}{c}[|\mathbf{r}_o - \mathbf{R}_1| + |\mathbf{R}_1 - \mathbf{r}_1|]$$

$$t_R = \frac{2}{c}[|\mathbf{r}_o - \mathbf{R}_2| + |\mathbf{r}_1 - \mathbf{R}_2| + (n-1)d]$$



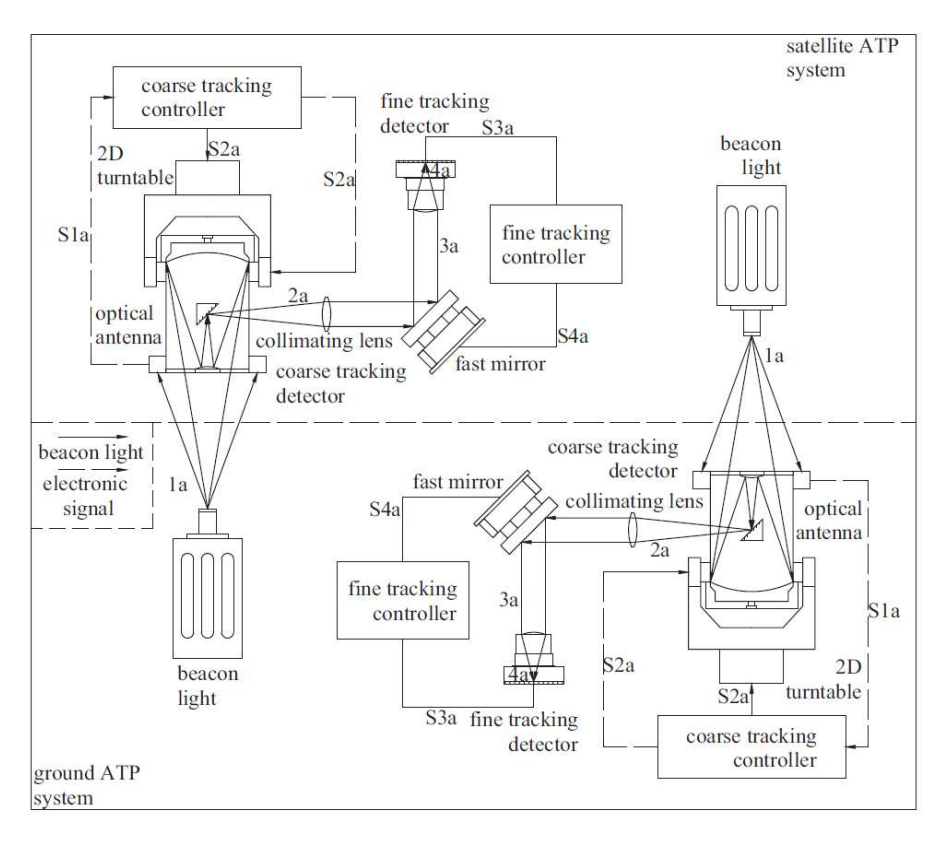
in which \mathbf{r}_o is the user position vector, \mathbf{R}_1 and \mathbf{R}_2 are the endpoints of the baseline, \mathbf{r}_1 is the position of the entangled photon source at the baseline, n and d are the effective refractive index and thickness of optical extension line. When the entangled photon pairs travel along the left and right paths of the baseline for the same time, **that is**, $\mathbf{t}_L = \mathbf{t}_R$, The interferometer has reached a state of equilibrium. At this juncture, the coincidence counting rate of the photon attains its minimum value. By measuring the time delay that coincides with the minimum in the coincidence counting rate, it is possible to determine the distance between the photon's trajectory and that of the user.

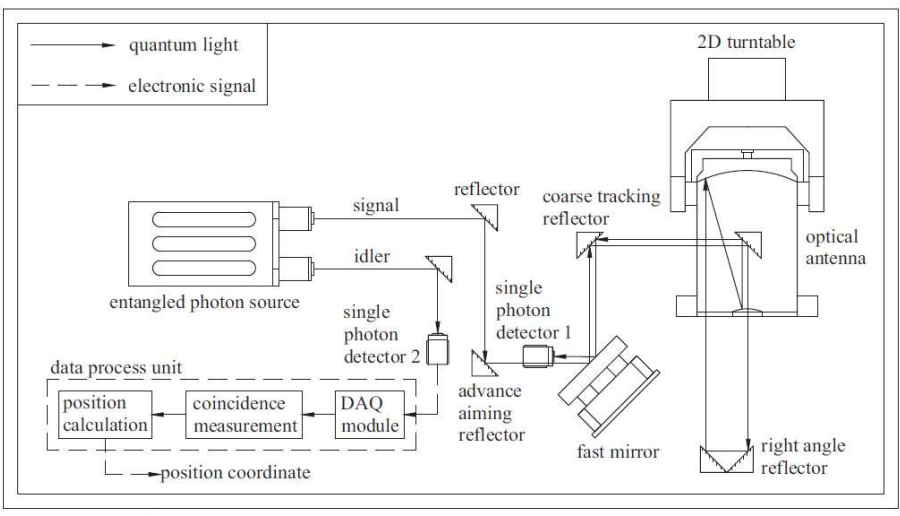
One of the most widely used schemes at present is quantum positioning technology based on six satellites.

Nevertheless, due to the considerable financial outlay required for the deployment of satellites and the finite resources available, a quantum positioning technology based on a smaller number of satellites is being proposed for a range of positioning and navigation tasks. In the context of autonomous navigation of a constellation of satellites, which differs from the

positioning and navigation of ground users, the number of satellites can be reduced to three. In 2014, Xiong et al. put forth a methodology for satellite ranging that employs a quantum light source and a reflection mirror on the satellite. In this approach, the quantum light source and measurement apparatus are mounted on the client satellite, enabling the generation and emission of entangled photon pulse signals. The reflector and pointing mechanism are installed on the beacon satellite with the purpose of reflecting the received signals to the client satellite. By measuring the time difference of arrival (TDOA) between the emitted and reflected entangled photon pulse signals, it is possible to achieve a high degree of accuracy in the measurement of distances between the client and beacon satellites. This method can be employed to achieve autonomous navigation of a satellite based on intersatellite distance measurement, thereby reducing the dependence of the satellite on ground control and enhancing the survival ability of the constellation system in an emergency.

In 2019, Cong et al. put forth a quantum positioning system (QPS) comprising three quantum satellites. The quantum light source, ATP system, photon interferometry system and signal processing system were studied in detail, and the results of this study provide a theoretical basis for the realization of the whole quantum positioning system. The process of quantum optical communication between a satellite and a ground user in this system is shown in the figures below, which are taken from reference [4].





In order to realize the positioning process of the ground user, the quantum signal is typically transmitted to the user and the time-difference-of-arrival (TDOA) value of the pulse signal is calculated in order to determine the position of the user. The entangled photon source transmits the entangled photon pair signal through a polarizing beam splitter (PBS), relaying it to two reference satellites in the baseline. The signal is then reflected back to the user through a reflector.

The user carries an angular reflector that returns the photon pair signal to the transmitter along the same path. With a 50:50 beam splitter, the photon signal is split and sent to two detectors for coincidence counting. The two optical signal paths are of equal length, with the exception of one path, which contains an optical delay unit to adjust the transmission time $\Delta t = (n-1)d/c$ in order for the two photons to reach the coincidence counting unit simultaneously, it is necessary for the Hong-Ou-Mandel (HOM) interferometer to reach an equilibrium state. In the aforementioned equation, d represents the geometric thickness of the adjustable optical delay unit, which is perpendicular to the light path. The effective refractive index of the optical delay unit, denoted by n, allows us to calculate the extra path length generated by the optical delay unit. = (n-1)d/c. The delay value of the optical delay unit is adjusted (usually by adjusting n) until the minimum counting rate is observed on the HOM interferometer.

The condition of the **minimum counting rate** is that the delay of the entangled photon pair traveling along the left and right paths is equal. The minimum value of two photon counting rate is unique, that is, it only corresponds to the delay value of the optical delay unit. The d and n of the adjustable optical delay unit **determine** its delay time Δt , which is the TDOA value between the baseline endpoints and the user's position. In the positioning process, three equations of the TDOA value are needed to solve the three-dimensional position coordinates of the user. For each equation, it has a distance of $c\Delta t$ generated by the optical delay unit and the distance can be replaced by (n-1)d in the equation, in which d can be measured through the delay unit. When the entangled photon source is in the user's part, the time synchronization of satellite and ground user is unnecessary.

In the event that the entangled photon source is situated at the satellite, it becomes necessary to introduce an additional fourth interferometer with the objective of synchronizing the user's clock with the satellite's clock.

The concept of quantum clock synchronization is derived from the phenomenon of quantum entanglement in pairs, such as photons or atoms. In contrast to the approach of observing the satellite simultaneously and resolving the discrepancy in position and clock time through the actions of the ground user,

the processes of positioning and clock synchronization are two distinct and independent procedures within the context of QPS. These procedures employ disparate implementation methodologies. By employing second-order quantum coherence, the discrepancy between the user's and the QPS's clocks, situated in close proximity to the origin of the coordinate system, is meticulously quantified, thereby enabling the user's clock to be synchronized with the system clock. The process of synchronizing the satellite base QPS does not require knowledge of the distance between the user and the system clock. Furthermore, it is noteworthy that QPS positioning and clock synchronization only necessitate short-term stability for the user clock and satellite-borne clock, with no long-term stability requirements. This is due to the fact that the two-photon consistent counting measurement employed by the HOM interferometer only necessitates that the clock be stable for a brief measuring period. Nevertheless, the system clock situated in close proximity to the origin of the coordinate system must exhibit robust long-term stability in order to ensure the maintenance of precise system time.

The satellite positioning system employs the time delay of the signals transmitted and received between the satellite and ground user as the fundamental observation variable, and utilizes this to calculate the distance between the two entities, thereby enabling the positioning process to be completed. It can be seen, therefore, that the accuracy of satellite and Earth clock synchronization has a significant impact on the positioning accuracy and reliability of satellite positioning. In order to maintain synchronization between the satellite clock and GPS time, classical methods employ a combination of clock error prediction, time contrast and carrier phase observation. The use of high-precision atomic clocks and clock difference prediction in classical methods can facilitate the attainment of time accuracy within a range of 6–10 ns. The unidirectional synchronization method proposed by Zhang can achieve an accuracy of 5–10 ns, while the accuracy of the bidirectional synchronization method can reach 1–2 ns. Furthermore, the laser synchronization method can achieve an accuracy of less than 1 ns. In 2010, Qu put forth a methodology

based on the dual-frequency carrier phase contrast, achieving an accuracy of 160 ps.

In the context of the nascent quantum positioning system, the quantum clock synchronization scheme put forth by Jozsa et al. in 2000 was founded upon the utilization of entangled quantum pairs. However, Yurtsever and Burt challenged the fundamental premise of the scheme, highlighting that the proposed QCS approach was incomplete. Concurrently, John put forth a quantum protocol for clock synchronization and evaluated potential avenues for enhancing its resilience through distillation entanglement and error correction.

Chuang of the IBM Almaden Research Centre put forth a distributed QCS algorithm, which is relatively intricate.

In 2004, Zhang et al. of Tsinghua University implemented the algorithm in a three-bit NMR quantum system experiment. In 2006, Wu et al. presented a scheme for implementing the algorithm using a linear optical method. In 2004, Valencia et al. demonstrated the principle of remote clock synchronization through an experiment based on entangled photon pairs. They used an optical fibre as the quantum transmission channel to conduct the quantum remote clock synchronization experiment and proposed a method that directly measured the second-order correlation of two entangled photons, circumventing the use of a HOM interferometer. The difference method allows for the calculation of clock differences with a picosecond resolution over a distance of 3 km; however, the scheme is susceptible to the influence of the dispersion effect. In the same year, Bahder employed a HOM interferometer to ascertain the time of reception of an entangled photon pair, following the adjustment of the optical path in order to achieve synchronization.

This method necessitates the calibration and measurement of the thickness of the delayed crystal in order to obtain the desired results. In 2011, Exman put forth a multi-QCS scheme based on n-particle w-state optimization. However, the preparation of an n-particle w-state is a challenging endeavour, which constrains the scope of this scheme's applicability. Xie put forth a theoretical framework for quantum clock synchronization, utilizing the structure of the Mach-Zender (MZ) interferometer. The phase difference between two photons

sent through an MZ interferometer can be used to calculate the clock difference. Given that the sensitivity is on the order of the wavelength, there is no requirement to set a physical clock and measure the arrival time of the pulse. Consequently, this method is not susceptible to the effects of gravitational potential, while simultaneously exhibiting resilience against the influences of dispersion, thereby enabling the fulfilment of heightened requirements. Nevertheless, this scheme necessitates the availability of two identical optical paths, which presents a significant challenge in the context of remote quantum teleportation. In 2014, Yang et al. put forth a synchronous measurement method for satellite-earth clocks based on a second-order correlation function. The method provides time accuracy of less than 140 fs, which can be applied in the synchronization process to enhance the time synchronization accuracy of QPS. In 2016, Quan et al. proposed a clock synchronization method based on second-order quantum interference and demonstrated its efficacy by applying this method to the synchronization of two clocks connected by an optical fibre 4 km apart, obtaining an absolute measurement accuracy of 73.2 picoseconds. The results demonstrate that this method can be applied to the synchronization of extremely accurate time systems.

References Chapter 2:

- [1] F. Steinlechner (2015), Sources of Photonic Entanglement for applications in Space
- [2] A. Belenchia et al. (2022), Quantum physics in space
- [3] Chao-Yang Lu rt al. (2022), Micius quantum experiments in space
- [4] Shiqi Duan, Shuang Cong and Yuanyuan Song (2020), A survey on quantum positioning system, International Journal of Modelling and Simulation
- [5] Donghui Feng (2019), Review of Quantum navigation, IOP Conference Series: Earth and Environmental Science
- [6] T. B. Bahder (2004), Quantum Positioning System
- [7] Daniel KL Oi et al. (2017), CubeSat quantum communications mission, EPJ Quantum Technology

CHAPTER 3

1. Introduction to Quantum Synchronization

A significant study has been conducted with the objective of enhancing satellite-based positioning through the utilization of quantum synchronization. The initial step is to differentiate between network-centric and user-centric positioning. These are distinct methodologies for determining the location of a user's device through radio signal measurements. In network-centric positioning, the process is under the responsibility of the network operator or service provider. The processing of uplink signals, as observed in the context of IoT devices, does not necessitate a significant amount of local computational power, resulting in a high degree of accuracy. Conversely, user-centric positioning necessitates the computation of downlink signals transmitted by the network infrastructure. The Global Navigation Satellite System (GNSS) can be classified as a user-centric positioning system.

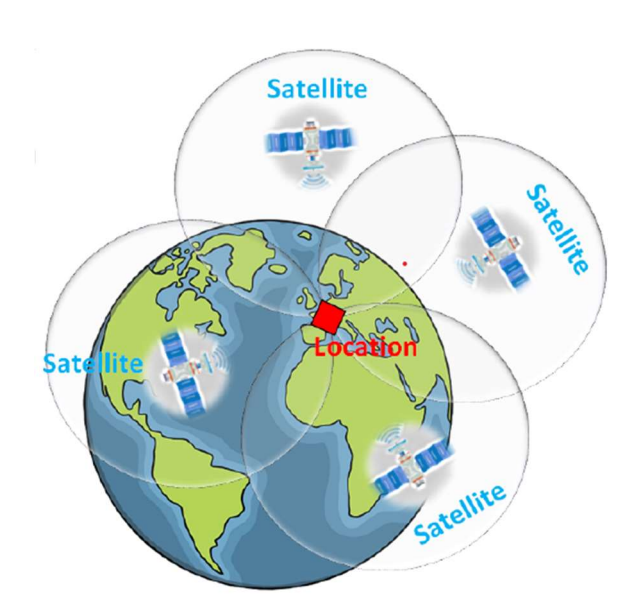
To accurately compute the distance between the navigation receiver and each GNSS satellite, time measurement techniques such as time of arrival (TOA) or time difference of arrival (TDOA) must be employed. A fundamental aspect of this process is the synchronization between GNSS satellites. Precise time synchronization and clock/frequency synchronization between navigation satellites is required for both user-side and network-side localization, employing frequency difference of arrival (FDOA). In this context, atomic clocks, which utilize the vibrations of atoms to measure time, play a pivotal role by providing highly accurate timekeeping on board GNSS satellites. Their operation is based on quantum transitions at microwave frequencies between hyperfine levels in the ground state of the atoms. However, atomic clocks are costly and have a relatively large size, which precludes their use on small, low-cost satellites. Quantum synchronization (QS) represents an intriguing novel approach to supporting satellite-based localization systems utilizing low-cost, compact satellites (e.g., CubeSats).

In classical systems, the process of synchronization entails the adjustment of an oscillator's rhythm in response to external perturbations, such as electromagnetic radiation. However, this approach frequently results in latency, which in turn leads to delays in the transmission of data and signals between devices. The use of atomic clocks, software-based solutions, and network time protocols (NTP) could potentially reduce latency and enhance accuracy. However, these methods are susceptible to electromagnetic interference (EMI), gravitational waves, and magnetic fields that could induce slight variations in atomic vibration. It is possible that vibrations and temperature fluctuations may exert an influence on atomic clocks. The integrity of GPS signals may be compromised by the presence of satellite signal interference, and the functionality of GPS receivers may be impaired by the introduction of noise and jitter. In both instances, the processes of timing and synchronization are affected. Furthermore, satellites are susceptible to impairment due to natural phenomena, such as the impact of solar wind, and are subject to maintenance and service disruptions. NTP can guarantee an accuracy of 10-100 milliseconds, which is well below the effective needs of high accuracy. QS is a process that uses quantum mechanics to synchronize clocks or other physical systems. It employs entangled particles or qubits to transmit quantum information between two clocks, which permits extremely accurate synchronization. A quantum-enabled GPS system could potentially achieve higher accuracy and robustness compared to traditional GPS systems.

In the absence of network node synchronization, the user equipment (EU) localization in three-dimensional space requires the computation of time of arrival (TOA) or time difference of arrival (TDOA) for each node. This is achieved through the formulation of a system of equations incorporating unknown coordinates and the synchronization error. This can be considered analogous to the study of the dynamics of four-qubits (one for each node) and the evolution of related quantum states. The synchronization of four qubits represents a frontier in the field of study. In this chapter, we consider a constellation of four satellites and investigate the positioning errors generated by the synchronization and ephemeris errors. Our findings suggest that QS systems

may achieve synchronization errors below one meter, which would result in a highly accurate location. **Quantum synchronization (QS)** is a phenomenon resulting from nonlinear interactions among quantum oscillators. It can be efficiently implemented in an optical lattice clock (OLC), which is a type of atomic clock that uses a lattice of photons to trap and cool atoms, allowing for extremely precise timekeeping. This result is a foundational one for metrological capabilities, with a fractional uncertainty of 2.0×10⁻¹⁷. It could allow the positioning of atomic clocks in space. When optical technologies, such as optical clocks, are added to this, the improvement in GNSS position determination is significant. The combination of optical clocks with optical inter-satellite communication implies a future where GNSS dependability and precision will be significantly enhanced.

In the case of traditional GNSS systems, the positioning is determined by a process known as **trilateration**. This is an algorithm that uses the distances between a point and several reference points to ascertain the position of the point in question. Typically, three or more known locations are considered in order to triangulate a position (see the figure below).



In order to calculate the distances in question, it is possible to utilize GPS technology. This would entail determining the centre of each sphere by

employing the measured distance and the coordinates of the reference point. Subsequently, the intersections of multiple spheres can be identified. It is necessary to eliminate any solutions that are incompatible with the physical constraints. It is necessary to reiterate the preceding steps.

The time of arrival (TOA) of a signal between a transmitter and a receiver can be calculated directly by multiplying the measured time taken for the signal to travel between them by the known propagation speed, which is typically the speed of light. It can be expressed in the following form:

$$TOA = t_u - t_s$$

Where u stand for user's side and s for satellite side. A minimum of three satellites are required to determine the unknown precision within the network. If the unknown position is denoted as (x_{ref}, y_{ref}) and the locations of the satellites is denoted as $(x_{s,j}, y_{s,j})$, then the distance from each of three satellites is the one below:

$$d_j = \sqrt{(x_{\text{ref}} - x_{s,j})^2 + (y_{\text{ref}} - y_{s,j})^2}$$

$$t_j = \frac{d_j}{c}; j = 1,2,3$$

A high degree of synchronization between the transmitter and receiver is required for precise TOA measurements.

The Time Difference of Arrival (TDOA) is the difference in arrival times at two transmitters, like below:

$$d_{j} - d_{j+1} = \sqrt{(x_{\text{ref}} - x_{s,j})^{2} + (y_{\text{ref}} - y_{s,j})^{2}} - \sqrt{(x_{\text{ref}} - x_{s,j+1})^{2} + (y_{\text{ref}} - y_{s,j+1})^{2}}$$

TDOA does not necessitate a direct line-of-sight path between the source and each receiver. Consequently, the algorithm can perform effectively in the

presence of physical obstructions and/or complex environments, including urban areas, where GPS signals could be impaired or weak. It is necessary to ensure synchronization among the receivers within the network.

In order to sustain system oscillations, QS operates with an equilibrium between energy absorption and dissipation. The principles of quantum mechanics are implicated. The incorporation of QS into satellite navigation systems demonstrates its capacity to revolutionize precision timing and positioning technologies. The consistent amplitude of limit cycle oscillations enables quantum oscillators to function as dependable reference signals for accurately determining satellite positions.

The free Hamiltonian H_0 of the system is defined below:

$$H_0 = \frac{\hbar\Omega}{2}\hat{\sigma}_z$$

Where Ω represent the frequency of Rabi oscillations and $\hat{\sigma}_z$ is the Pauli's z-operator. The synchronization of the qubits' phase to the external field's frequency is governed by the following law:

$$\widehat{H}_{Rabi} = -\hbar\Omega \left(e^{-i\varphi_j}|0\rangle\langle 1| + e^{i\varphi_j}|1\rangle\langle 0|\right)$$

2. Novel technique for QS

According to literature, the Tavis-Cummings Hamiltonian for a four-qubit system is the following:

$$\begin{split} \widehat{H} &= \hbar \omega_0 \left(\widehat{n} + \frac{1}{2} \right) + \sum_{i=1}^4 \frac{\hbar \Omega_i}{2} \widehat{\sigma}_z^{(i)} \\ &+ g \hbar \omega_0 \sum_{i=1}^4 \widehat{\sigma}_x^{(i)} (\widehat{a} + \widehat{a}^\dagger) + f \cos \left(\omega t \right) (\widehat{a} + \widehat{a}^\dagger) \end{split}$$

Integrating the resonator's frequency ω_0 , each qubit's Rabi frequency Ω_i , their respective Pauli operators. g is the coupling constant between the qubit and the photon. The annihilation and creation operators \hat{a} and \hat{a}^{\dagger} , respectively. $f=\hbar\lambda\sqrt{n_p}$ is the driving force amplitude (n_p is the number of photons in the

resonator at the resonance $\omega=\omega_0$, where g=0). λ is the dissipation rate in the resonator

In this context, the **Lindblad master equation (LME)** is employed to ascertain the spectral density, which signifies the synchronization of the qubits. The evolution of our system, which accounts for dissipation effects, is accurately modelled by the master equation:

$$\frac{d}{dt}\hat{\rho} = \frac{1}{i\hbar}[\hat{H},\hat{\rho}] + \frac{\lambda}{2}(2\hat{a}\hat{\rho}\hat{a}^{\dagger} - \hat{a}^{\dagger}\hat{a}\hat{\rho} - \hat{\rho}\hat{a}\hat{a}^{\dagger})$$

The first term on the right-hand side represents the unitary evolution of the system, described by the Hamiltonian \widehat{H} . The second, third, and fourth terms on the right-hand side represent the dissipative interactions between the system and its environment.

This equation is critical for understanding the QS in our system, taking into account both coherent interactions and the unavoidable fact of dissipation. *LME* can be employed to identify the conditions under which synchronization occurs and analyse the stability of synchronized states

The spectral density $S(\omega)$ is indispensable for analyzing the energy distribution across frequencies within our four-qubit satellite system, offering crucial insights into the QS dynamics. $S(\omega)$ is essential for understanding how coupled qubits interact and synchronize with each other.

Defined by the Fourier transform (it is employed to convert time-domain data into frequency-domain data) of the autocorrelation function of an observable, the spectral density for our system described by the raising and lowering operators $\sigma_+(t)$ and $\sigma_-(t)$, is mathematically expressed as:

$$S(\omega) = \int_{-\infty}^{\infty} e^{-i\omega t} \langle \sigma_{+}(t)\sigma_{-}(0) + \sigma_{-}(t)\sigma_{+}(0) \rangle dt$$

The expectation value, $\langle ... \rangle$, encompasses the dynamics of the quantum state and interactions with external fields. This equation facilitates the exploration of resonance phenomena and energy exchange mechanisms, which are critical

for evaluating the efficiency and stability of synchronization across the satellite network. A coupling strength that is neither very strong nor very weak is referred to as having a weak coupling strength. In the context of quantum computing, this approach is often preferred due to the fact that weak coupling helps to minimize the loss of quantum coherence that would otherwise occur as a result of unwanted interactions with the surrounding environment. The spectral density S(v) of the system comprising four qubits as a function of the coupling strength f(g) is illustrated in the diagram below.

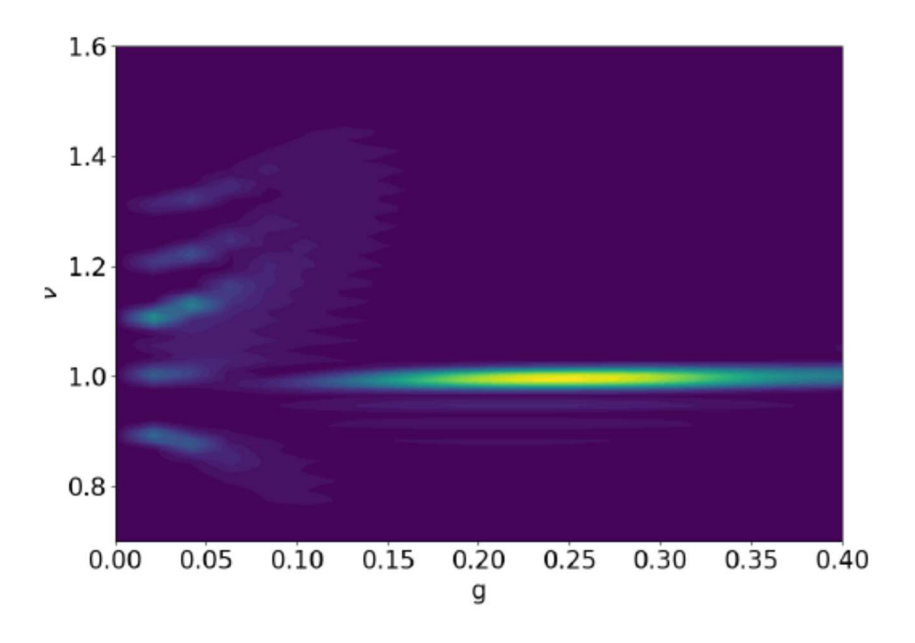


Figure from [1]

As clearly seen in this figure, the qubits are not synchronized when g is varied between 0.0 and 0.10. However, they are synchronized when $g \in [\sim 0.12, \sim 0.40]$ with frequency of $\nu = 1$. The synchronization of the four-qubits is confirmed by computing the expectation values of spin operators $\langle \hat{\sigma}_x \rangle$ over time ℓ . This synchronization is of great importance for the coordinated functioning of quantum systems and forms the basis for the development of advanced quantum network capabilities.

It is envisaged that a constellation of four satellites, each containing a single qubit, will be used to determine the position of the UE. The satellites are connected by optical inter-satellite links (ISLs), which serve two purposes: high-

bandwidth data communication and QS. The complete systematic representation is provided in figure below:

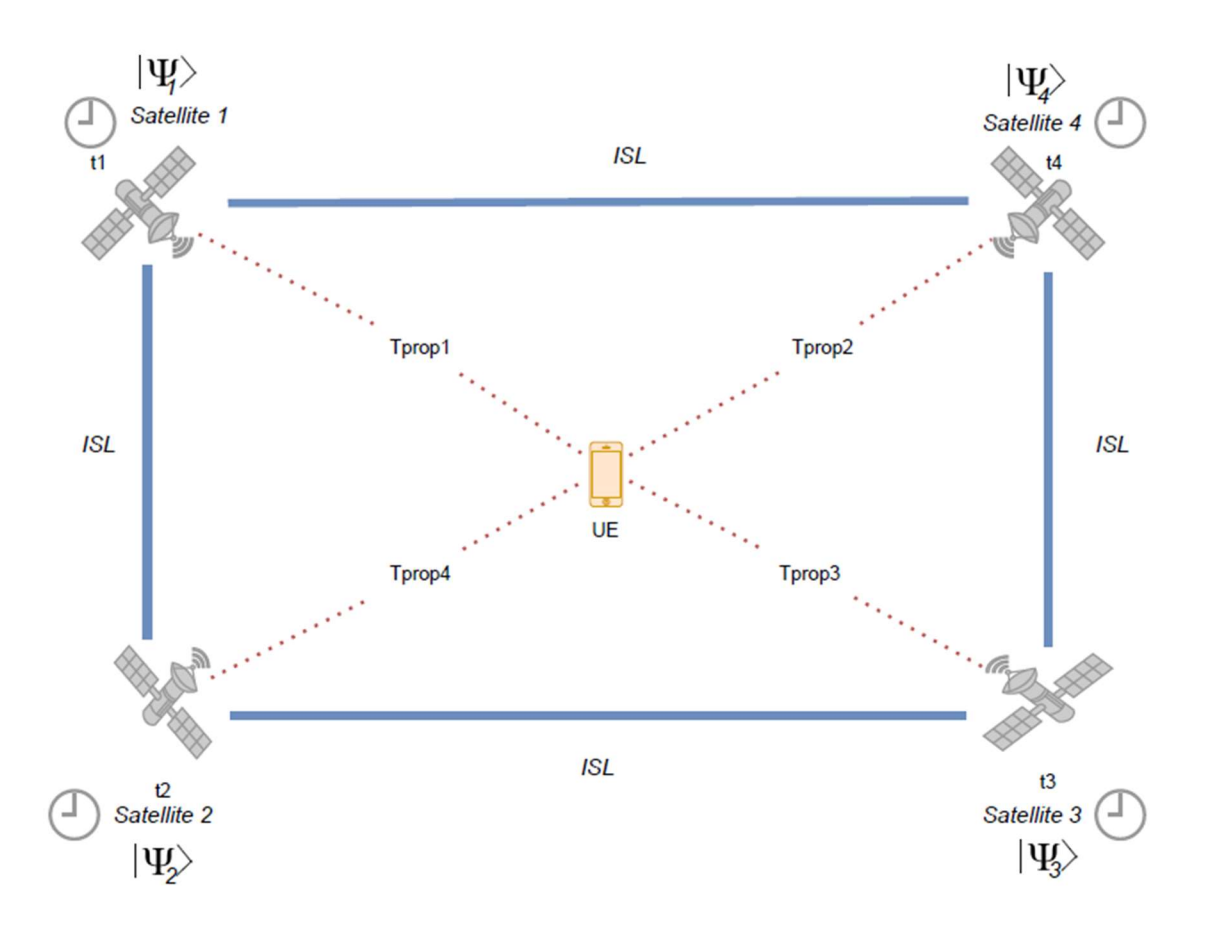


Fig. from [1]

The initial stage of the experiment involved simulating the synchronization of four qubits using ISL links among the four satellites, which were designated as $|\psi_1\rangle, |\psi_2\rangle, |\psi_3\rangle, |\psi_4\rangle$. Second, by employing the Lindblad Master Equation and the Hamiltonian Equation, it was possible to achieve a coherent synchronization state across the qubits. This was verified through spectral density analysis, which demonstrated that a robust quantum entanglement network had been established.

Subsequently, the UE transmits signals to all four satellites, which then identify the time of arrival (TOA) of the signals. The total time of arrival (TOA) at each specific satellite is defined as the time reference t_j , where j denotes the index

of the satellite. This value is then added to the propagation time, denoted as $t_{prop,j}$. Indeed, the user equipment (UE) transmits a signal to the satellite that is geographically closest to it, which then receives the signal via the satellite's transponder. Subsequently, the signal is amplified and transmitted to the subsequent satellite in the constellation. As the user equipment (UE) relocates from one geographical area to another, it will transfer its connection from one satellite to another. This process is referred to as a handover or handoff. The UE will perform a continuous assessment of the signal strength and quality from each satellite, selecting the optimal one to maintain communication.

Subsequently, the signal is transmitted from the second satellite to the third, and so forth, until it reaches its final destination. The ISL facilitates data transfer between satellites, thereby enabling efficient communication.

All satellites execute an algorithm, such as trilateration, in order to calculate the position and identify the unknown location of the UE.

The satellite then assesses the performance and identifies any errors based on the calculated position.

By reducing the occurrence of synchronization errors, investigators can enhance the frequency stability of quantum atomic clocks, allowing them to maintain their accuracy over longer periods and thereby increasing their value for applications such as timekeeping and synchronization. To illustrate, the frequency stability of quantum atomic clocks utilizing 87 Sr necessitates a precision of approximately 2.2×10^{-18} at 1 second.

The synchronization process is initiated with the following steps:

- From the outset, the ISLs synchronize the qubits across the satellites, thereby forming a unified quantum state that spans the constellation.
- Dynamical Evolution: The evolution of this entangled state over time is modelled using the Lindblad master equation, which incorporates both the qubits' internal dynamics and their ISL-mediated interactions.

The role of feedback and control in this process is as follows: Real-time feedback mechanisms are employed to dynamically adjust the Hamiltonian's parameters, such as k_{ij} , based on the continuous monitoring of the qubits' states, with the objective of sustaining or enhancing the synchronization.

The technical considerations encompass a range of factors, including optical ISL, environmental decoherence, and real-time quantum state monitoring. LEO constellations of small satellites represent the optimal implementation for this framework. Given the range of potential synchronization errors, which encompass QS systems and ns-grade atomic clocks on board satellites, simulations have been conducted to assess position accuracy (see the figure below). The results demonstrate that satisfactory outcomes can be attained. When satellites are synchronized through a quantum approach with a synchronization error below 0.01 ns, the resulting positioning error may be lower than 1 m, contingent on the error associated with the satellite position.

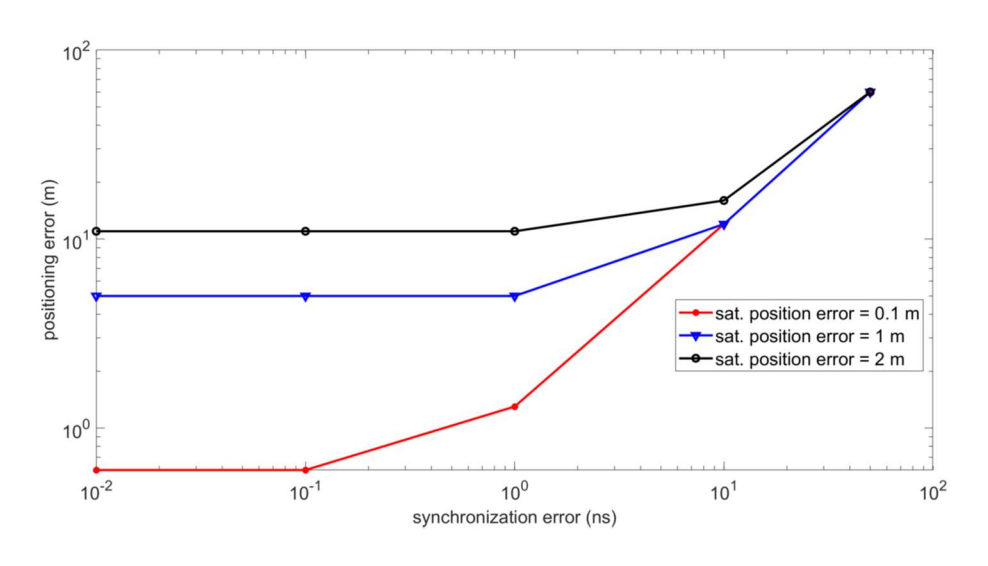


Figure from [1]

A further technique has been proposed by Wei He, Yong Wang in [2]. They put forth an efficacious and resilient entangled photons-based positioning system (EPPS), wherein a framework for the categorization and selection of signal and idle photons is proposed with the objective of achieving a balance between effectiveness and accuracy. A signal propagation model for entangled photons has been developed which takes into account a number of factors, including

noise, the number of emitted photons and detection efficiency. The model is used to analyze the reasons affecting the number of detected photons.

Based on the Cramer-Rao Lower Bound (CRLB) of the range accuracy with various grouping factors, they propose a rapid data grouping and selection algorithm. An enhanced simulated annealing (SA) algorithm is integrated with CRLB calculation to rapidly identify the optimal grouping strategy for diverse scenarios and select multiple groups for target range estimation. This approach strikes a balance between precision and efficiency in the positioning system.

In light of the potential failure of the access point (AP) to capture the target during positioning (e.g., due to AP malfunction), a fusion positioning method is proposed to ensure robust localization in dynamic environments. Furthermore, extensive experiments have been conducted on the entangled photons positioning platform to verify the effectiveness and robustness of the proposed system.

3. Conclusion and outlook

The current state of research in the field of quantum positioning systems (QPS) is still in its early stages of development. Since the initial theoretical work was conducted in 2001, numerous advancements have been made, yet a fully space-based operational system remains an unfulfilled objective. In contrast, the initial passive systems have been deployed, and their development has progressed in parallel with that of the broader quantum sensing discipline. Although it is unlikely that the space-based quantum positioning system will supplant the classical positioning systems in the near future, the continuous progress of various related disciplines will undoubtedly precipitate a revolution in the field of positioning technology. It is a daring conjecture that the implementation of quantum technology in a classical positioning system will result in a notable enhancement in performance.

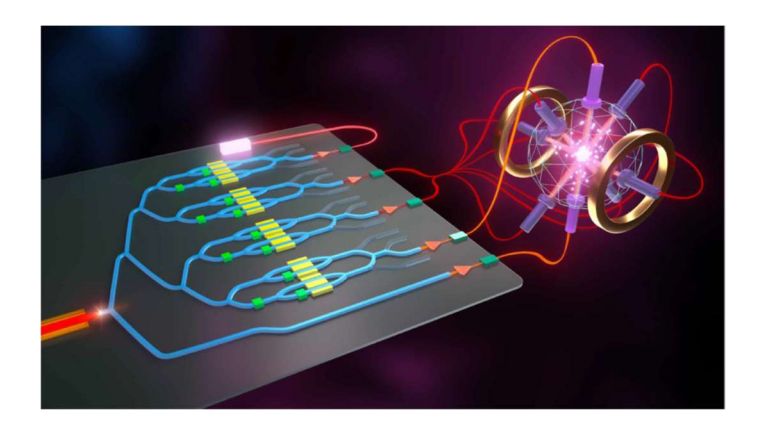
As a novel, precise positioning technology distinct from classical GPS, the QPS represents a paradigm shift in the integration of quantum optics and contemporary positioning technology.

Further research into this technology may facilitate the development of nextgeneration positioning systems with enhanced precision, particularly in the following areas; the advancement of theorical approach and novel techniques and engineering implementation will usher in the quantum era for electronic information systems. In the practical implementation of quantum technology, high-performance and large-scale quantum devices have emerged, including satellite-earth quantum secure communication, quantum computing processing units, and high-performance entanglement sources. This also provides a solid foundation for the eventual implementation of quantum positioning technology. Moreover, the integration of quantum positioning and cryptography may prove to be the most effective approach for making the space-based QPS a practical reality in the future. At the present time, quantum cryptography represents the most practical technology among those currently in use. The combination of the space-based QPS with quantum cryptography allows for the expansion of the system's functionality and the enhancement of its security and anti-interference capabilities.

The QPS, based on quantum mechanics, has the potential to surpass the limitations of classical measurement, achieving enhanced accuracy.

The accelerated advancement of quantum information technology has facilitated the growth of technologies pertaining to the fabrication, manipulation and storage of quantum devices and quantum signals (e.g. quantum repeaters). The resolution of these issues will provide robust technical support for the investigation of a quantum positioning system. In light of the constraints currently impeding the advancement of this field, the construction of a comprehensive system framework is among the first. The theoretical framework should include, but not be limited to, the following elements: entanglement preparation scheme, satellite baseline setup, angular reflector, HOM interferometer, coincidence counter, anti-noise measures, and multi-user protocol, among others. Photonic integrated circuits may give a hand to reduce

dimensions of devices. Many advances have been done recently. See, for example, High-performance silicon photonic single-sideband modulators for cold-atom interferometry in [3], figure below:



Maintenance of entanglement state of quantum signal plays a key role. The transmission of quantum signals over long distances may present challenges in maintaining the coherence and stability of entangled photon pairs.

Integration of quantum and classical positioning technologies is another important issue. The development of quantum positioning systems is a lengthy process, given the maturation of current positioning technologies.

Recently, a proposal to leverage optical ISLs for the dual purpose of high-bandwidth data communication and Quantum Synchronization (QS), thereby supplanting atomic clocks with QS systems has arisen, following the current trend to design satellite constellations that can perform both communications and positioning services. It is important to consider the potential challenges of applying quantum synchronization in real-world systems, due to the noise present in space, which can affect the stability of entangled particles and compromise the precision of measurements. One significant challenge to QS is the distance between the satellites and the maintenance of a stable connection of the entanglement signal, which diminishes with increasing distance. But intellectual and financial huge investments are necessary. These investments are essential for the advancement of theoretical and applied research, as well as for the development of prototypes and the industrialisation of processes, in order to facilitate the future creation of operational, active space-based quantum processing systems. It seems reasonable to suppose that these systems will be

capable of functioning not only in satellites with dedicated payloads, su ch as CubeSats or nanosatellite constellations, but also, in the longer term,in high-altitude platforms (HAP) and unmanned aerial vehicles (UAVs). Such developments will facilitate the advent of cooperative intelligent transportation systems (C-ITS), connected automated vehicles (CAV), and an array of Internet of Things (IoT) devices and other "things" in the ocean.

References Chapter 3

- [1] S.S. Nande, T. Rossi, M.I. Habibie et al., Satellite-based positioning enhanced by quantum synchronization, Computer Networks, 2024
- [2] Wei He, Yong Wang, An Efficient and Robust Fusion Positioning System Based on Entangled Photons, IEEE Journal on selected areas in communications, 2024
- [3] Ashok Kodigala et al., High-performance silicon photonic single-sideband modulators for cold-atom interferometry, Science Advances, 2024